Laboratory of Biopharmaceutical Research[1], National Institute of Biomedical Innovation; Laboratory of Toxicology and Safety Science[2], Graduate School of Pharmaceutical Sciences; The Center for Advanced Medical Engineering and Informatics[3]; Laboratory of Biomedical Innovation[4], Graduate School of Pharmaceutical Sciences, Osaka University, Osaka, Japan

Rho GDP-dissociation inhibitor alpha is associated with cancer metastasis in colon and prostate cancer

T. YAMASHITA[1,2,*], T. OKAMURA[1,*], K. NAGANO[1,*], S. IMAI[1], Y. ABE[1], H. NABESHI[1,2], T. YOSHIKAWA[1,2], Y. YOSHIOKA[1,2,3], H. KAMADA[1,3], Y. TSUTSUMI[1,2,3], S. TSUNODA[1,3,4]

Received July 7, 2011, accepted August 5, 2011

Shin-ichi Tsunoda, Ph.D, Laboratory of Biopharmaceutical Research, National Institute of Biomedical Innovation, 7-6-8 Saito-Asagi, Ibaraki, Osaka 567-0085, Japan.
tsunoda@nibio.go.jp
**These authors contributed equally to the work.*

Pharmazie 67: 253–255 (2012) *doi: 10.1691/ph.2012.1630*

Since metastasis is one of the most important prognostic factors in colorectal cancer, development of new methods to diagnose and prevent metastasis is highly desirable. However, the molecular mechanisms leading to the metastatic phenotype have not been well elucidated. In this study, a proteomics-based search was carried out for metastasis-related proteins in colorectal cancer by analyzing the differential expression of proteins in primary versus metastasis focus-derived colorectal tumor cells. Protein expression profiles were determined using a tissue microarray (TMA), and the results identified Rho GDP-dissociation inhibitor alpha (Rho GDI) as a metastasis-related protein in colon and prostate cancer patients. Consequently, Rho GDI may be useful as a diagnostic biomarker and/or a therapeutic to prevent colon and prostate cancer metastasis.

1. Introduction

Colorectal cancer is known as a major metastatic cancer, and 40–50% of patients already have a metastatic focus at presentation. Moreover, the 5-year survival of these patients is under 10% (Davies et al. 2005). Thus, metastasis is one of the most important prognostic factors in colorectal cancer. In order to improve rates of cancer remission, it will be necessary to clarify the detailed molecular mechanisms of cancer metastasis and to utilize this information to establish new diagnostic and therapeutic techniques. Many researchers have searched for metastasis-related molecules (Liu et al. 2010; Shuehara et al. 2011) using proteomics techniques (Hanash 2003). Comprehensive mapping of the molecular changes during metastasis would greatly improve our understanding of the recurrence and management of cancer. However, the knowledge gained so far in these studies has not been sufficient to improve cancer remission rates.

Here we show the potential of Rho GDI as a metastasis-related protein in colon and prostate cancer patients. In order to identify metastasis-related proteins, the protein expression patterns of human colorectal cancer cells with different metastatic characters were compared. Because these cells were derived from the same patient (SW480: a surgical specimen of a primary colon adenocarcinoma, SW620: a lymph node metastatic focus), cancer metastasis-related protein candidates could be effectively sought without background variations due to differences between individuals. Furthermore, by analyzing the expression of candidate proteins in many clinical samples using a TMA, we attempted to validate the association of these candidates with metastasis. TMA is a slide glass containing many clinical tissues, and it enables one to carry out a high-throughput analysis by evaluating the relationship between expression profiles of each candidate molecule and clinical information such as metastasis. (Imai et al. 2011; Yoshida et al. 2011).

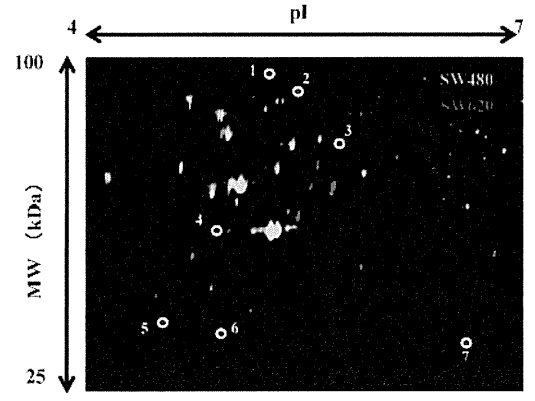

Fig. 1: 2D-DIGE image of fluorescently-labeled proteins from different metastatic human colorectal cancer cells. SW480 is human colorectal cancer cell line derived from a primary tumor and SW620 is derived from a metastatic focus from the same patient. Proteins from the colon cancer cells (SW480, SW620) were labeled with Cy3 and Cy5 respectively, and analyzed by 2D electrophoresis. The differentially-expressed spots (white circles) were then identified by LC-UHR TOF/MS

Table 1: High expression proteins in SW620 compared to SW480

	Accession	Protein name	MW (kDa)	pI	Ratio (SW620 / SW480)
1	P12109	collagen alpha-1(VI) chain	108.6	5.3	1.53
2	Q15459	splicing factor 3A subunit 1	88.9	5.2	1.61
3	P13797	T-plastin	70.9	5.5	1.59
4	P60709	actin cytoplasmic 1	42.1	5.3	1.50
5	P63104	14-3-3 zeta/delta	27.9	4.7	1.63
6	P52565	Rho GDP-dissociation inhibitor 1 (Rho GDI)	23.3	5.0	1.90
7	P30041	Peroxiredoxin-6 (PRDX6)	25.1	6.0	1.86

2. Investigations, results and discussion

In order to search for metastasis-related proteins, we analyzed differentially-expressed proteins between SW480 and SW620 by two-dimensional differential in-gel electrophoresis (2D-DIGE) (Fig. 1). As a result, 7 spots with at least a 1.5-fold-altered expression level were found by quantitative analysis, and these spots were identified by mass spectrometry (Table 1). Three molecules having a high SW620/SW480 expression ratio indicating a strong association with cancer metastasis were identified: Rho GDP-dissociation inhibitor alpha (Rho GDI), peroxiredoxin-6 (PRDX6) and 14-3-3 zeta/delta.

The expression profiles of these proteins were analyzed by immunohistochemistry using the TMA with colon cancer and multiple cancer tissues. Results of this analysis indicated that expression of PRDX6 and 14–3-3 zeta/delta had no relationship to the clinical status of cancer metastasis (data not shown). On the other hand, in positive cases of lymph node metastasis, the expression ratio of Rho GDI was significantly higher than in the negative cases. Furthermore, the same trend was seen when tissues from prostate cancer patients were analyzed (Table 2).

To confirm these results, the expression levels of Rho GDI protein in colon cancer cell lines with different metastatic potential (SW480 < SW620 < SW620-OK1 < SW620-OK2: Characteristics of SW620-OK1 and SW620-OK2 are described in *Experimental*) were investigated by western blot analysis (Fig. 2). The expression of Rho GDI was found to be up-regulated with the development of metastatic characteristics. These results suggested that Rho GDI is correlated with cancer metastasis.

Rho GDI has been identified as key regulator of Rho family GTPases. Activation of growth factor receptors and integrins can promote the exchange of GDP for GTP on Rho proteins (Bishop et al. 2000). Furthermore, GTP-bound Rho proteins interact with a range of effector molecules to modulate their activity or localization, and this leads to changes in cell behavior. It is clear that Rho family GTPases are involved in the control of cell morphology and motility (Etienne-Manneville et al. 2002; Hall et al. 1997; Van Aelst et al. 1997). The importance of Rho protein and Rho GDI in cancer progression, particularly in the area of metastasis, is becoming increasingly evident. Recently, some reports have indicated that the expression of Rho GDI was correlated with colorectal and breast cancer metastasis (Zhao et al. 2008; Kang et al. 2010). Thus, our findings are consistent with these reports and further suggest that the expression of Rho GDI is also correlated with prostate cancer metastasis. Consequently, Rho GDI should be considered as a diagnostic marker or new therapeutic target for cancer metastasis.

3. Experimental

3.1. Cell lines

SW480 is a human colorectal cancer cell line derived from a primary focus and SW620 is derived from a metastatic focus of the same patient. These cells were purchased from American Type Culture Collection and maintained at 37 °C using Leibovitz's L-15 medium (Wako) supplemented with 10% FCS. SW620-OK1 and -OK2 were established by the following procedure: 1×10^6 SW620 cells were injected into the spleens of nu/nu mice. After 8 weeks, SW620-OK1 was established from a liver metastatic focus. Furthermore, SW620-OK2 was established from SW620-OK1 using the same procedures.

3.2. 2D-DIGE analysis

Cell lysates were prepared from SW480 and SW620 and then solubilized with 7 M urea, 2 M thiourea, 4% CHAPS and 10 mM Tris-HCl (pH 8.5). The lysates were labeled at the ratio of 50 μg proteins: 400 pmol Cy3 or Cy5 protein-labeling dye (GE Healthcare Biosciences) in dimethylformamide according to the manufacturer's protocol. Briefly, the labelled samples were mixed with rehydration buffer (7 M urea, 2 M thiourea, 4% CHAPS, 2% DTT, 2% Pharmalyte (GE Healthcare Biosciences)) and applied to a 24-cm immobilized pH gradient gel strip (IPG-strip pH 4–7 NL) for separation in the first dimension. Samples for the spot-picking gel were prepared without labelling by Cy-dyes. For the second dimension separation, the IPG-strips were applied to SDS-PAGE gels (10% polyacrylamide and 2.7% N,N'-diallyltartardiamide gels). After electrophoresis, the gels were scanned with a laser fluoroimager (Typhoon Trio, GE Healthcare Biosciences). The spot-picking gel was scanned after staining with Deep Purple Total Protein Stain (GE Healthcare Biosciences). Quantitative analysis of protein spots was carried out with Decyder-DIA software (GE Healthcare Biosciences). For the antigen spots of interest, spots of 1 mm × 1 mm in size were picked using Ettan Spot Picker (GE Healthcare Biosciences).

3.3. In-gel tryptic digestion

Picked gel pieces were digested with trypsin as described below. The gel pieces were destained with 50% acetonitrile/50 mM NH_4HCO_3 for 20 min twice, dehydrated with 75% acetonitrile for 20 min, and then dried using a centrifugal concentrator. Next, 5 μl of 20 μl/ml trypsin (Promega) solution was added to each gel piece and incubated for 16 h at 37 °C. Three solutions were used to extract the resulting peptide mixtures from the gel pieces. First, 50 μl of 50% (v/v) acetonitrile in 0.1% (v/v) formic acid (FA) was added to the gel pieces, which were then sonicated for 5 min. Next, we collected the solution and added 80% (v/v) acetonitrile in 0.1% FA. Finally, 100% acetonitrile was added for the last extraction. The peptides were dried and then re-suspended in 10 μl of 0.1% FA.

3.4. Mass spectrometry and database search

Extracted peptides were analyzed by liquid chromatography Ultra High Resolution time-of-flight mass spectrometry (LC-UHR TOF/MS; maXis, Bruker Daltonics). The Mascot search engine (http://www.matrixscience.com) was initially used to query the entire theoretical tryptic peptide database as well as SwissProt (http://www.expasy.org/, a public domain database pro-

Table 2: Expression profile of Rho GDI in primary cancers with or without lymph node metastasis

	Number of Rho GDI positive cases (positive ratio)	
	in metastasis negative cases	in metastasis positive cases
Colon cancer*	11/14 (79%)	19/19 (100%)
Prostate cancer*	18/23 (78%)	11/11 (100%)

* $p < 0.05$: Mann Whitney U test

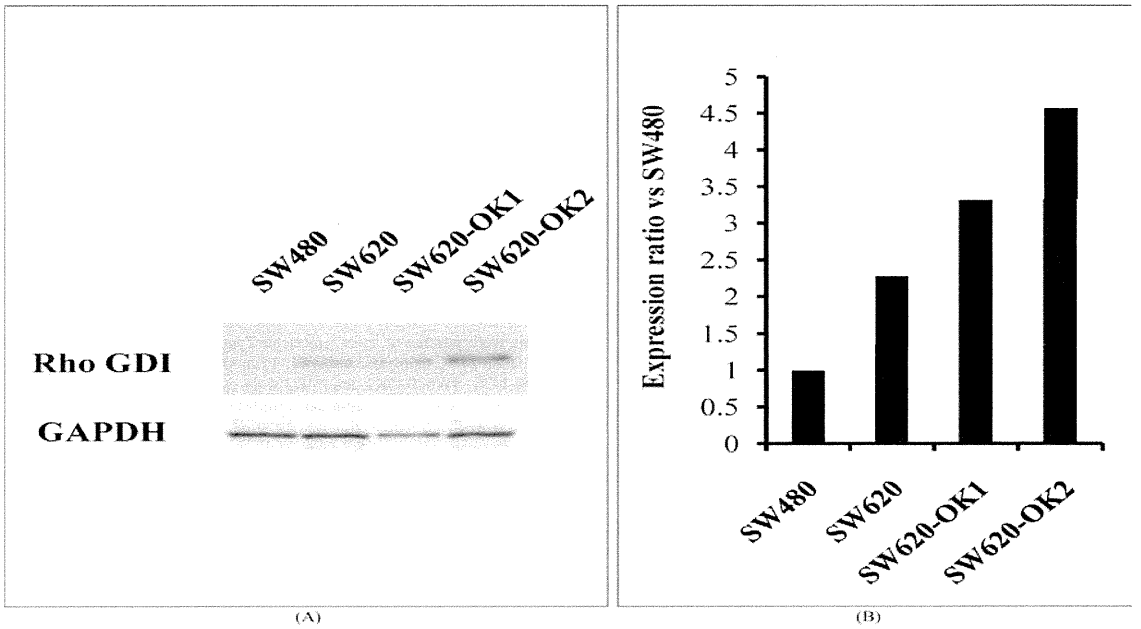

Fig. 2: Rho GDI expression levels in colon cancer cell lines with different metastatic abilities. Rho GDI expression levels in colon cancer cell lines (SW480, SW620, SW620-OK1, SW620-OK2) analyzed by western blotting (A). SW620-OK1, SW620-OK2 have been established as high metastatic sub-lines of SW620 using a mouse metastasis model. Intensity of the western blotting images was quantified by densitometry (B)

vided by the Swiss Institute of Bioinformatics). The search query assumed the following: (i) the peptides were monoisotopic (ii) methionine residues may be oxidized (iii) all cysteines are modified with iodoacetamide.

3.5. TMA Immunochemical staining

TMA slides with human colon cancer samples or multiple cancer samples (Biomax) were de-paraffinated in xylene and rehydrated in a graded series of ethanol washes. Heat-induced epitope retrieval was performed while maintaining the Target Retrieval Solution pH 9 (Dako) at the desired temperature according to manufacturer's instructions. After the treatment, endogenous peroxidase was blocked with 0.3% H_2O_2 in Tris-buffer saline (TBS) for 5 min. After washing twice with TBS, TMA slides were incubated with 10% BSA blocking solution for 30 min. The slides were then incubated with the anti-Rho GDI (Santa Cruz Biotechnology) for 60 min. After washing three times with wash buffer (Dako), each series of sections was incubated for 30 min with Envision + Dual Link (Dako). The reaction products were rinsed twice with wash buffer and then developed in liquid 3, 3'-diaminobenzidine (Dako) for 3 min. After the development, sections were counterstained with Mayer's hematoxylin. All procedures were performed using AutoStainer (Dako).

3.6. TMA Immunohistochemistry scoring

The optimized staining conditions for TMAs corresponding to human colon as well as multiple cancers were determined based on the co-existence of both positive and negative cells in the same tissue sample. Signals were considered positive when reaction products were localized in the expected cellular component. The criteria for scoring of stained tissues were as follows: the distribution score was 0 (0%), 1 (1–50%) or 2 (51–100%), indicating the percentage of positive cells among all tumor cells present in one tissue. The intensity of the signal (intensity score) was scored as 0 (no signal), 1 (weak), 2 (moderate) or 3 (marked). The distribution and intensity scores were then summed into a total score (TS) of TS0 (sum = 0), TS1 (sum = 2), TS2 (sum = 3), and TS3 (sum = 4–5). Throughout this study, TS0 or TS1 was regarded as negative, whereas TS2 or TS3 were regarded as positive.

3.7. Western Blot

Expression of Rho GDI in colon cancer cells was detected by anti-Rho GDI (Santa Cruz Biotechnology) and HRP conjugated anti-mouse IgG antibody (Sigma) using the ECL-plus system. Equal amounts of protein loading were confirmed by parallel β-actin immunoblotting, and signal quantification was performed by densitometric scanning.

Acknowledgements: This study was supported in part by Grants-in-Aid for Scientific Research from the Ministry of Education, Culture, Sports, Science and Technology of Japan, and from the Japan Society for the Promotion of Science (JSPS). This study was also supported in part by Health Labor Sciences Research Grants from the Ministry of Health, Labor and Welfare of Japan.

References

Bishop AL, Hall A (2000) Rho GTPases and their effector proteins. Biochem J 348: 241–255.

Davies RJ, Miller R, Coleman N (2005) Colorectal cancer screening: prospects for molecular stool analysis. Nat Rev Cancer 5: 199–209.

Etienne-Manneville S, Hall A (2002) Rho GTPases in cell biology. Nature 420: 629–635.

Hall A (1997). Rho GTPases and the Actin cytoskeleton. Science 279: 509–514.

Hanash S (2003) Disease proteomics. Nature 422: 226–232.

Imai S, Nagano K, Yoshida Y, Okamura T, Yamashita T, Abe Y, Yoshikawa T, Yoshioka Y, Kamada H, Mukai Y, Nakagawa S, Tsutsumi Y, Tsunoda S (2011). Development of an antibody proteomics system using a phage antibody library for efficient screening of biomarker proteins. Biomaterials 32: 162–169.

Kang S, Kim MJ, An H, Kim BG, Choi YP, Kang KS, Gao MQ, Park H, Na HJ, Kim HK, Yun HR, Kim DS, Cho NH (2010) Proteomic molecular portrait of interface zone in breast cancer. J Proteome Res 9: 5638–5645.

Liu R, Wang K, Yuan K, Wei Y, Huang C (2010) Integrative oncoproteomics strategies for anticancer drug discovery. Expert Rev Proteomics 7: 411–429.

Sahai E (2007). Illuminating the metastatic process. Nat Rev Cancer 7: 737–749.

Suehara Y, Tochigi N, Kubota D, Kikuta K, Nakayama R, Seki K, Yoshida A, Ichikawa H, Hasegawa T, Kaneko K, Chuman H, Beppu Y, Kawai A, Kondo T (2011) Secernin-1 as a novel prognostic biomarker candidate of synovial sarcoma revealed by proteomics. J Proteomics 74: 829–842.

Van Aelst L, D'Souza-Schorey C (1997) Rho GTPases and signaling networks. Genes Dev 11: 2295–2322.

Yoshida Y, Yamashita T, Nagano K, Imai S, Nabeshi H, Yoshikawa T, Yoshioka Y, Abe Y, Kamada H, Tsutsumi Y, Tsunoda S (2011) Limited expression of reticulocalbin-1 in lymphatic endothelial cells in lung tumor but not in normal lung. Biochem Biophys Res Commun 405: 610–614.

Zhao L, Wang H, Li J, Liu Y, Ding Y (2008) Overexpression of Rho GDP-dissociation inhibitor alpha is associated with tumor progression and poor prognosis of colorectal cancer. J Proteome Res 7: 3994–4003.

Biochemical and Biophysical Research Communications 421 (2012) 140–144

Contents lists available at SciVerse ScienceDirect

Biochemical and Biophysical Research Communications

journal homepage: www.elsevier.com/locate/ybbrc

Annexin A4 is a possible biomarker for cisplatin susceptibility of malignant mesothelioma cells

Takuya Yamashita [a,b,1], Kazuya Nagano [a,1], So-ichiro Kanasaki [a,b], Yuka Maeda [a,b], Takeshi Furuya [a,b], Masaki Inoue [a], Hiromi Nabeshi [b], Tomoaki Yoshikawa [a,b], Yasuo Yoshioka [a,b,c], Norio Itoh [b], Yasuhiro Abe [a], Haruhiko Kamada [a,c], Yasuo Tsutsumi [a,b,c], Shin-ichi Tsunoda [a,c,d,*]

[a] Laboratory of Biopharmaceutical Research, National Institute of Biomedical Innovation, 7-6-8 Saito-Asagi, Ibaraki, Osaka 567-0085, Japan
[b] Laboratory of Toxicology and Safety Science, Graduate School of Pharmaceutical Sciences, Osaka University, 1-6 Yamadaoka, Suita, Osaka 565-0871, Japan
[c] The Center for Advanced Medical Engineering and Informatics, Osaka University, 1-6 Yamadaoka, Suita, Osaka 565-0871, Japan
[d] Laboratory of Biomedical Innovation, Graduate School of Pharmaceutical Sciences, Osaka University, 1-6 Yamadaoka, Suita, Osaka 565-0871, Japan

ARTICLE INFO

Article history:
Received 27 March 2012
Available online 4 April 2012

Keywords:
Malignant mesothelioma
Cisplatin susceptibility
Annexin A4
Biomarker
Proteomics

ABSTRACT

Mesothelioma is a highly malignant tumor with a poor prognosis and limited treatment options. Although cisplatin (CDDP) is an effective anticancer drug, its response rate is only 20%. Therefore, discovery of biomarkers is desirable to distinguish the CDDP-susceptible versus resistant cases. To this end, differential proteome analysis was performed to distinguish between mesothelioma cells of different CDDP susceptibilities, and this revealed that expression of annexin A4 (ANXA4) protein was higher in CDDP-resistant cells than in CDDP-susceptible cells. Furthermore, ANXA4 expression levels were higher in human clinical malignant mesothelioma tissues than in benign mesothelioma and normal mesothelial tissues. Finally, increased susceptibility was observed following gene knockdown of ANXA4 in mesothelioma cells, whereas the opposite effect was observed following transfection of an ANXA4 plasmid. These results suggest that ANXA4 has a regulatory function related to the cisplatin susceptibility of mesothelioma cells and that it could be a biomarker for CDDP susceptibility in pathological diagnoses.

1. Introduction

Malignant mesothelioma is an aggressive neoplasm located on serosal membrane surfaces such as the pleura, and less frequently the peritoneum, and it has a poor outcome. The five-year survival rate is only about 5%. On the other hand, it is well known that asbestos is the major causative agent in the development of this disease [1–3]. Moreover, malignant mesothelioma takes 40–50 years to develop following exposure to asbestos. Because of its adiabatic potential, asbestos was commonly used as a building material in the 1960–1970s. Thus, an increase in mesothelioma patients is expected in the future. Patients with pleural malignant mesothelioma commonly present with an effusion associated with breathlessness that is often accompanied by chest-wall pain and a cough. After confirming the diagnosis, many patients are treated by intensive multidirectional approaches that combine cytoreductive surgery with intrapleural or intraperitoneal chemotherapy [4–8]. However, cytoreductive surgery is not always possible for patients with extensive intraperitoneal disease. Thus, the role of chemotherapy in malignant mesothelioma is critically important.

CDDP is an extensively used anticancer drug for the treatment of malignant mesothelioma, although the response rate is only about 20% [9–12]. A major problem with CDDP treatment of malignant mesothelioma patients is the development of CDDP insusceptibility. Thus, there is an urgent need to further our understanding of the pathogenesis of malignant mesothelioma, particularly with respect to the expression of proteins that confer drug susceptibility, in order to develop novel therapeutic strategies. In this study, a proteomic analysis was performed using high- and low-CDDP-susceptible malignant mesothelioma cells to identify candidate proteins associated with CDDP susceptibility.

2. Materials and methods

2.1. Cells

H28, H2052, H2452, H226 and MSTO-221H were purchased from American Type Culture Collection and maintained in RPMI1640 medium (Wako) containing 10% fetal calf serum (Biowest). Human mesothelial cells (HMC) were purchased from

* Corresponding author at: Laboratory of Biopharmaceutical Research, National Institute of Biomedical Innovation, 7-6-8 Saito-Asagi, Ibaraki, Osaka 567-0085, Japan. Fax: +81 72 641 9817.
E-mail address: tsunoda@nibio.go.jp (S.-i. Tsunoda).
[1] These authors contributed equally to this work.

0006-291X/$ - see front matter © 2012 Elsevier Inc. All rights reserved.
http://dx.doi.org/10.1016/j.bbrc.2012.03.144

Sciencell and cultured in Mesothelial Cell Growth Medium (ZenBio) under a 5% CO_2 atmosphere at 37 °C.

2.2. Measurement of cisplatin susceptibility in malignant mesothelioma cells

Malignant mesothelioma cells were seeded into 96-well microplates and cultured overnight. Various concentrations of CDDP were added to each well, the plates were incubated for 24 h, and cell viability was measured using Cell count reagent SF (Nacalai tesque). Absorbance was measured using a microplate reader (Bio-Rad) at test and reference wavelengths of 450 and 650 nm, respectively.

2.3. Proteomic analysis using two dimensional differential in-gel electrophoresis

For proteomic analysis, quantitative analysis was performed using two dimensional differential in-gel electrophoresis (2D-DIGE). Cell lysates were prepared from H28 and H2052 and then solubilized with 7 M urea, 2 M thiourea, 4% CHAPS and 10 mM Tris–HCl (pH 8.5). The lysates were labeled at the ratio of 50 μg proteins: 400 pmol Cy3 or Cy5 protein-labeling dye (GE Healthcare Biosciences) in dimethylformamide according to the manufacturer's protocol. The labelled samples were mixed with rehydration buffer (7 M urea, 2 M thiourea, 4% CHAPS, 2% DTT, 2% Pharmalyte (GE Healthcare Biosciences)) and applied to a 24-cm immobilized pH gradient gel strip (IPG-strip pH 4–7) for separation in the first dimension. For the second dimension separation, the IPG-strips were treated with iodoacetamide and applied to SDS–PAGE gels (10% polyacrylamide and 2.7% *N,N′*-diallyltartardiamide gels). After electrophoresis, the gels were scanned with a laser fluoroimager (Typhoon Trio, GE Healthcare Biosciences). The spot-picking gel was scanned after staining with Deep purple total protein stain (GE Healthcare Biosciences). Quantitative analysis of protein spots was carried out with Decyder-DIA software (GE Healthcare Biosciences). For the antigen spots of interest, spots of 1 mm × 1 mm in size were picked using Ettan Spot Picker (GE Healthcare Biosciences).

2.4. In-gel tryptic digestion

Picked gel pieces were destained with 50% acetonitrile/50 mM NH_4HCO_3 for 20 min twice, dehydrated with 75% acetonitrile for 20 min, and then dried using a centrifugal concentrator. Five microliter of 20 μg/ml trypsin (Promega) solution was added to each gel piece and the pieces were incubated for 16 h at 37 °C. The digested peptides were extracted sequentially using 50%, 80%, and 100% acetonitrile and then dried before being suspended in 10 μl of 0.1% formic acid.

2.5. Mass spectrometry and database search

Extracted peptides were analyzed by liquid chromatography ultra high resolution time-of-flight mass spectrometry (LC-UHR TOF-MS/MS; maXis, Bruker Daltonics). The Mascot search engine (http://www.matrixscience.com) was initially used to query the entire theoretical tryptic peptide database as well as SwissProt (http://www.expasy.org/, a public domain database provided by the Swiss Institute of Bioinformatics). The search query assumed the following: (i) the peptides were mono-, di- or tri-isotopic, (ii) methionine residues may be oxidized, (iii) all cysteines were modified with carbamidomethyl.

2.6. Western blot

The cell lysates were separated in 10% SDS–polyacrylamide gels and transferred to Immobilon membranes (Millipore). After blocking by 4% block ace (DS Pharma Biomedical) for 1 h at room temperature, the blots were reacted with primary antibodies in a buffer containing 0.4% block ace, and then with the appropriate peroxidase-conjugated secondary antibodies in the same buffer. Expression of ANXA4 in malignant mesothelioma cells was detected by mouse anti-human ANXA4 (Abnova: 1D3) followed by an HRP-conjugated anti-mouse IgG antibody (Sigma–Aldrich) using the ECL-plus system (GE Healthcare Biosciences). Equal amounts of protein loading were confirmed by parallel β-actin immunoblotting, and signal quantification was performed by densitometric scanning.

2.7. Immunohistochemistry staining

Human mesothelioma and normal tissue sections were deparaffinated in xylene and rehydrated in a graded series of ethanol dilutions. Heat-induced epitope retrieval was performed by incubating at different temperatures following the manufacturer's instructions using Target Retrieval Solution pH 9 (Dako). After heat-induced epitope retrieval treatment, endogenous peroxidase was blocked with a peroxidase blocking reagent (Dako). Following peroxidase blocking, the slides were incubated with 10% bovine serum albumin (BSA) solution for 30 min at room temperature. The slides were then incubated for 60 min with anti-human ANXA4 monoclonal antibody (9 μg/ml) in 3% BSA at room temperature. After washing 3 times with wash buffer (Dako), the slides were incubated for 30 min with ENVISION + Dual Link (Dako) at room temperature. They were then washed final 3 times and stained with 3,3′-diaminobenzidine. After development, the slides were lightly counterstained with Mayer's hematoxylin and mounted with resinous mounting medium.

2.8. Cisplatin susceptibility in cells transfected with ANXA4-siRNA and ANXA4-plasmid

H28 was transfected with ANXA4-siRNA (target sequence: AAGGATATCACAGAAGGATAT, Qiagen) using Hyperfect reagent (Qiagen) according to the manufacturer's instructions. In contrast, H2052 was transfected with ANXA4-pcDNA 3.1 (a gift from Naka T: Laboratory for Immune Signal, National Institute of Biomedical Innovation) using FuGENE HD transfection reagent (Roche). After transfection, the cells were treated with various concentrations of CDDP for 36 h (ANXA4-siRNA) or 24 h (ANXA4-pcDNA 3.1). Cell viability was measured as described above.

2.9. Statistical analysis

Differences in tumor volumes between the control and target groups were compared using the unpaired Student's *t*-test.

3. Results

3.1. CDDP susceptibility in malignant mesothelioma cells

Cell viability following CDDP treatment was examined to determine which cell lines had higher or lower susceptibility to CDDP. Among five tested mesothelioma cell lines, H2052 was the most and H28 the least susceptible cell line (Fig. 1). The IC_{50} values of H28, H2052, H2452, H226 and MSTO-221H were 154.5, 27.8, 66.0, 87.5 and 49.5 μM, respectively.

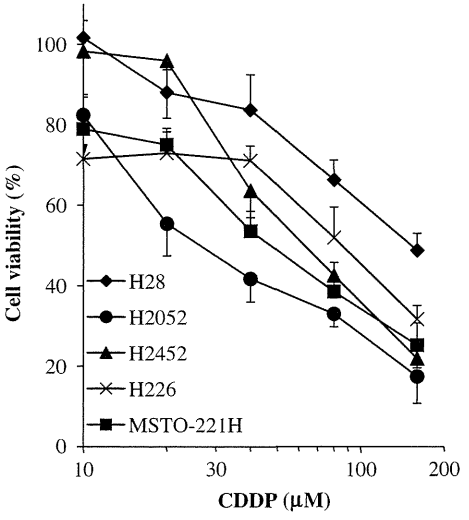

Fig. 1. Susceptibility of malignant mesothelioma cells to CDDP. Mesothelioma cells, H28, H2052, H2452, H226 and MSTO-221H were cultured with various concentrations of CDDP for 24 h 37 °C under 5% CO_2. Cell viability was assayed using the WST-8 assay. Maximal cell viability (100%) was obtained by incubating cells without CDDP. Data are shown as means and standard deviations ($n = 4$).

3.2. Identification of differentially expressed proteins by 2D-DIGE and MS

In order to search for CDDP susceptibility-related proteins, differential proteome analysis between H2052 and H28 cell lines was performed to search for CDDP susceptibility-related proteins (Fig. 2). Quantitative image analysis indicated that a total of eight protein spots representing > 2.0-fold alteration in expression were found and then identified by MS analysis (Table 1). Among those eight proteins, we focused on ANXA4 because this protein plays an important role in membrane stability. Previous reports have indicated that ANXA4 is associated with chemoresistance against platinum-based anticancer drugs in human lung, colon [13] and ovarian cancer [14].

3.3. ANXA4 expression analysis in human malignant mesothelioma cells and mesothelial tissues

Correlations between the expression levels in five malignant mesothelioma cell lines with CDDP-susceptibility were examined using western blot analysis to validate the identified proteins as CDDP susceptibility-related proteins. ANXA4 was expressed at a higher level in H28 cells relative to the other four CDDP-susceptible malignant mesothelioma cell lines (Fig. 3A and B). Expression of ANXA4 in human mesothelial tissue was analyzed by immunohistochemistry staining with an anti-human ANXA4 monoclonal antibody. Fig. 3C indicates that ANXA4 was expressed at higher levels in human malignant mesothelioma tissues than in benign mesothelioma tissues and normal mesothelial tissues.

3.4. Gene regulation of ANXA4 in malignant mesothelioma cells by knockdown and overexpression

ANXA4-siRNA and ANXA4-pcDNA 3.1 were next transfected to H28 and H2052 before CDDP treatment to evaluate correlations between ANXA4 expression levels and CDDP susceptibility. The IC_{50} values of [H28/non treat: H28/control-siRNA: H28/ANXA4-siRNA] were [80.0 μM: 71.8 μM: 15.5 μM] and [H2052/control-pcDNA 3.1: [H2052/ANXA4-pcDNA 3.1] were [55.2 μM: 89.7 μM], respectively (Fig. 4A–D). These results suggested that the CDDP susceptibility of H28 cells was increased by ANXA4-siRNA transfection and that of H2052 cells was decreased by ANXA4-pcDNA 3.1 transfection.

4. Discussion

In this study, a proteomic analysis was performed based on 2D-DIGE using malignant mesothelioma cell lines to identify candidate proteins associated with CDDP susceptibility (Figs. 1 and 2). Eight proteins that were differentially expressed in H28 cells compared with H2052 cells were identified (Table 1). ANXA4 was found to be expressed at a higher level in H28 cells relative to levels in CDDP-susceptible malignant mesothelioma cells by western blot

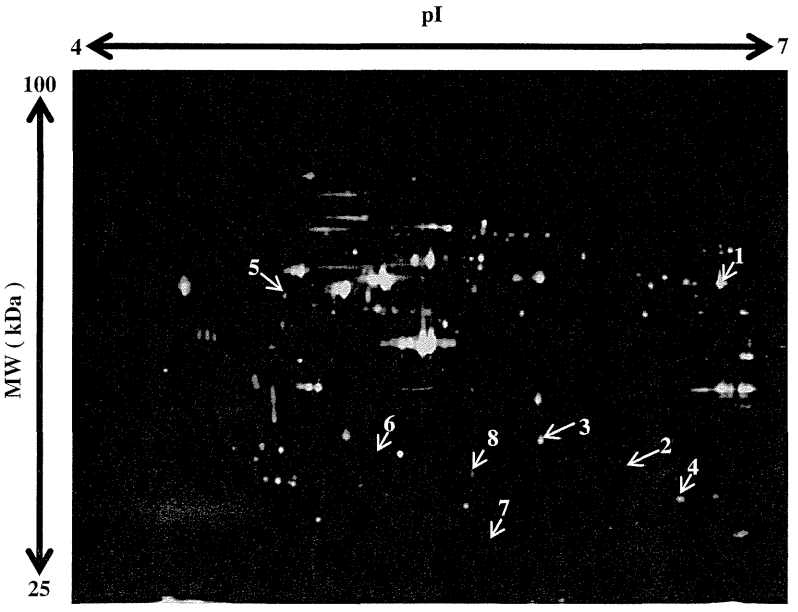

Fig. 2. 2D-DIGE image of fluorescently labeled proteins from human mesothelioma cell lines H28 and H2052. Proteins from high- and low-susceptible mesothelioma cells (H2052, H28) were labeled with cy3 and cy5, respectively, and 2D electrophoresis was performed. The differentially expressed spots in H28 indicated by white arrows were then identified by LC-TOF-MS/MS. Table 1 contains additional information about the identified proteins.

Table 1
Proteins expressed at higher or lower levels in H28 compared to H2052.

No.	Accession number	Protein name	pI	MW (kDa)	Expression ratio (H28/H2052)
1	P11413	Glucose-6-phosphate 1-dehydrogenase	6.4	59.3	21.0
2	P78417	Glutathione *S*-transferase omega-1	6.2	27.6	7.4
3	P09525	Annexin A4	5.6	35.9	3.6
4	P30041	Peroxiredoxin-6	6.0	25.0	3.5
5	Q09028	Histone-binding protein RBBP4	4.7	47.7	3.0
6	P07195	L-lactate dehydrogenase B chain	5.7	36.6	2.9
7	P32119	Peroxiredoxin-2	5.7	21.9	0.03
8	Q9Y696	Chloride intracellular channel protein 4	5.5	28.8	0.13

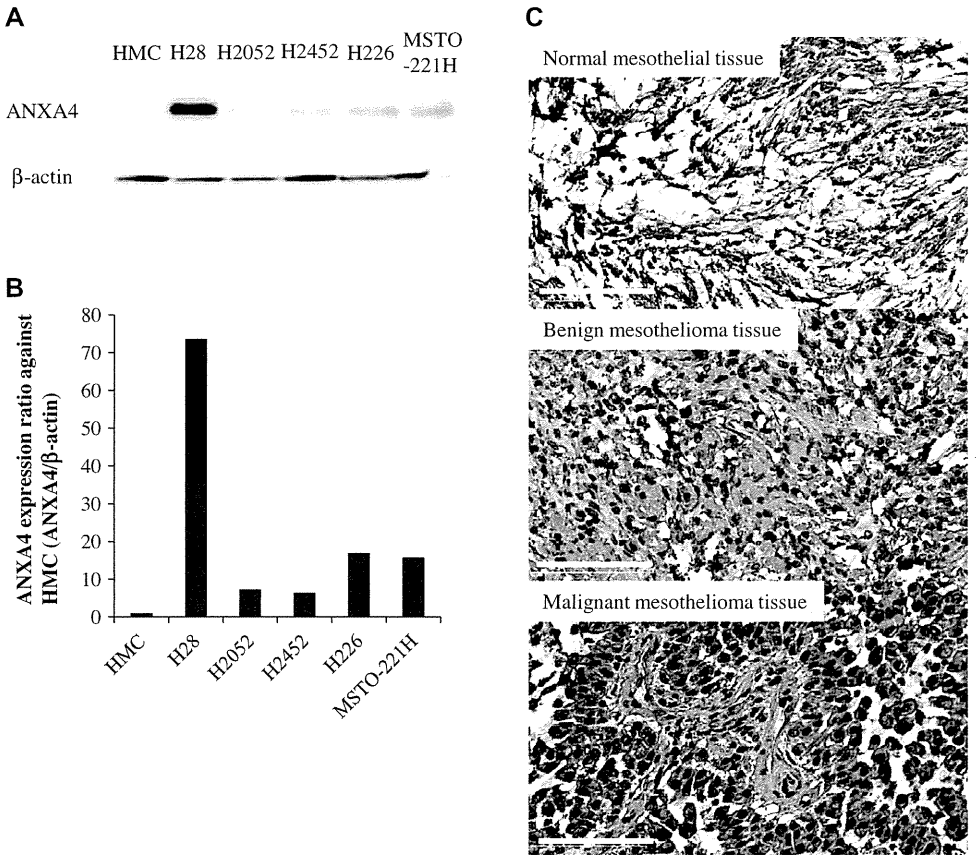

Fig. 3. ANXA4 expression analysis in human malignant mesothelioma cells and mesothelial tissues. ANXA4 expression levels in human primary mesothelial cells, HMC, and mesothelioma cell lines (H28, H2052, H2452, H226, MSTO-221H) were analyzed by western blotting (A). Intensity of the western blotting images was quantified by densitometry (B). Expression of ANXA4 in human mesothelial tissues was analyzed by immunostaining using an anti-human ANXA4 antibody (C). Top, middle and bottom panels are normal mesothelial, benign and malignant mesothelioma tissues, respectively. The tissue sections were counterstained using hematoxylin. Representative 400 × photomicrographs presented (bar: 100 μm).

analysis (Fig. 3A and B). Furthermore, ANXA4 was expressed in malignant mesothelioma tissue but not in benign mesothelial tumor and normal mesothelial tissues (Fig. 3C). Thus, ANXA4 was expressed in CDDP-susceptible malignant mesothelioma cells and specifically in malignant mesothelioma tissues. These results indicate that ANXA4 expression in malignant mesothelioma cells may be correlated with CDDP susceptibility, although this relationship must be validated in future studies of human clinical malignant mesothelial cases. The CDDP susceptibility of H28 cells was actually increased by ANXA4 knockdown, and that of H2052 cells was decreased by ANXA4 overexpression (Fig. 4). Thus, these results suggest that ANXA4 plays an important role in chemoresistance against CDDP.

ANXA4 has already been characterized as a regulator of cell membranes with calcium dependency [15–17]. Recently, some studies have reported the protein is associated with membrane permeability [18], ion channels [19] and exocytosis [20,21]. These observations may explain in part the correlation of ANXA4 with modulation of drug susceptibility in cancer cells.

This study demonstrates for the first time elevated ANXA4 protein expression in malignant mesothelioma cells that have less susceptibility to CDDP. *In vitro* evaluation of drug susceptibility against CDDP in malignant mesothelioma cells derived from cancer patients would be important in clinical conditions because doctors as well as patients wish to avoid treatment with inefficacious drugs. Consequently, the susceptibility of a given patient against CDDP could be confirmed by analyzing the expression level of ANXA4 in malignant mesothelioma patients at the time of diagnosis. Furthermore, if ANXA4 expression could be blocked specifically in malignant mesothelioma cells by nucleic acid drugs such as siRNA, this procedure would prove useful in clinical situations involving CDDP treatment. The present study may contribute to

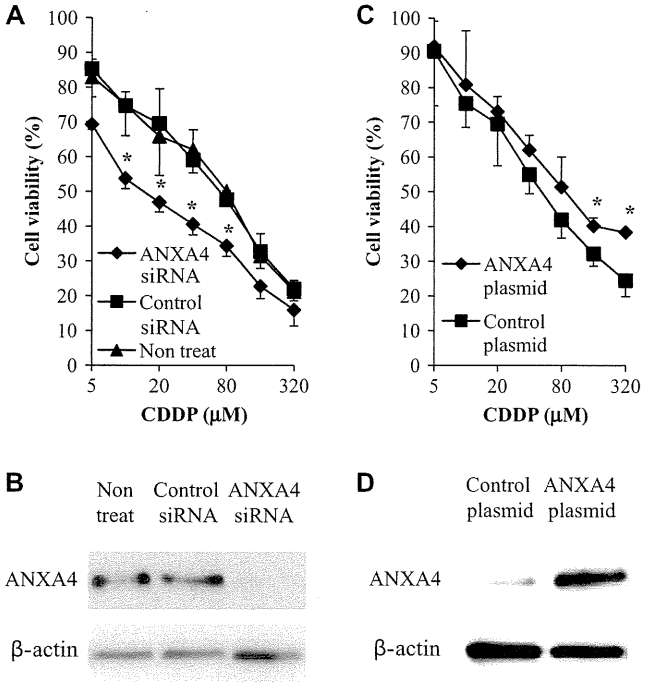

Fig. 4. The effect of ANXA4 gene knockdown and overexpression on CDDP susceptibility in malignant mesothelioma cells. Transfection of ANXA4 siRNA or plasmid into malignant mesothelioma cells confers resistance to CDDP. Cell survival after 24 h treatment of H28/ANXA4 siRNA or H2052/ANXA4 plasmid with different concentrations of CDDP (A and C). Expression of ANXA4 was analyzed by western blot analysis (B and D). Data are shown as means and standard deviations ($n = 4$). *$P < 0.05$ (Control siRNA or plasmid vs. ANXA4 siRNA or plasmid).

establishment of a new therapeutic strategy for malignant mesothelioma patients by suggesting a novel diagnostic and therapeutic target.

Acknowledgments

This study was supported in part by Grants-in-Aid for Scientific Research from the Ministry of Education, Culture, Sports, Science and Technology of Japan, and from the Japan Society for the Promotion of Science (JSPS). This study was also supported in part by Health Labor Sciences Research Grants from the Ministry of Health, Labor and Welfare of Japan and by Health Sciences Research Grants for Research on Publicly Essential Drugs and Medical Devices from the Japan Health Sciences Foundation.

References

[1] W.N. Rom, W.D. Travis, A.R. Brody, Cellular and molecular basis of the asbestos-related diseases, Am. Rev. Respir. Dis. 143 (1991) 408–422.
[2] N.H. Heintz, Y.M. Janssen-Heininger, B.T. Mossman, Asbestos, lung cancers, and mesotheliomas: from molecular approaches to targeting tumor survival pathways, Am. J. Respir. Cell Mol. Biol. 42 (2010) 133–139.
[3] Consensus Report: Asbestos, asbestosis, and cancer: the Helsinki criteria for diagnosis and attribution. Scand. J. Work Environ. Health 23 (1997) 311–316.
[4] T.D. Yan, L. Welch, D. Black, P.H. Sugarbaker, A systematic review on the efficacy of cytoreductive surgery combined with perioperative intraperitoneal chemotherapy for diffuse malignancy peritoneal mesothelioma, Ann. Oncol. 18 (2007) 827–834.
[5] E. Chailleux, D. Pioche, S. Chopra, G. Dabouis, P. Germaud, A.Y. De Lajartre, M. De Lajartre, Prognostic factors in diffuse malignant pleural mesothelioma: a study of 167 patients, Chest 93 (1988) 159–162.
[6] K.S. Sridhar, R. Doria, W.A. Raub Jr., R.J. Thurer, M. Saldana, New strategies are needed in diffuse malignant mesothelioma, Cancer 70 (1992) 2969–2979.
[7] M. Markman, D. Kelsen, Efficacy of cisplatin-based intraperitoneal chemotherapy as treatment of malignant peritoneal mesothelioma, J. Cancer Res. Clin. Oncol. 118 (1992) 547–550.
[8] G.H. Eltabbakh, M.S. Piver, R.E. Hempling, F.O. Recio, M.E. Intengen, Clinical picture, response to therapy, and survival of women with diffuse malignant peritoneal mesothelioma, J. Surg. Oncol. 70 (1999) 6–12.
[9] T. Berghmans, M. Paesmans, Y. Lalami, I. Louviaux, S. Luce, C. Mascaux, A.P. Meert, J.P. Sculier, Activity of chemotherapy and immunotherapy on malignant mesothelioma: a systematic review of the literature with meta-analysis, Lung. Cancer 38 (2002) 111–121.
[10] H.J. Lerner, D.A. Schoenfeld, A. Martin, G. Falkson, E. Borden, Malignant mesothelioma: The Eastern Cooperative Oncology Group (ECOG) experience, Cancer 52 (1983) 1981–1985.
[11] D.M. Mintzer, D. Kelsen, D. Frimmer, R. Heelan, R. Gralla, Phase II trial of high-dose cisplatin in patients with malignant mesothelioma, Cancer Treat Rep. 69 (1985) 711–712.
[12] B.L. Zidar, S. Green, H.I. Pierce, R.W. Roach, S.P. Balcerzak, L. Militello, A phase II evaluation of cisplatin in unresectable diffuse malignant mesothelioma: a Southwest Oncology Group Study, Invest New Drugs 6 (1988) 223–226.
[13] E.K. Han, S.K. Tahir, S.P. Cherian, N. Collins, S.C. Ng, Modulation of paclitaxel resistance by annexin IV in human cancer cell lines, Br. J. Cancer 83 (2000) 83–88.
[14] A. Kim, T. Enomoto, S. Serada, Y. Ueda, T. Takahashi, B. Ripley, T. Miyatake, M. Fujita, C.M. Lee, K. Morimoto, M. Fujimoto, T. Kimura, T. Naka, Enhanced expression of Annexin A4 in clear cell carcinoma of the ovary and its association with chemoresistance to carboplatin, Int. J. Cancer 125 (2009) 2316–2322.
[15] M.A. Kaetzel, P. Hazarika, J.R. Dedman, Differential tissue expression of three 35-kDa annexin calcium-dependent phospholipid-binding proteins, J. Biol. Chem. 264 (1989) 14463–14470.
[16] G. Zanotti, G. Malpeli, F. Gliubich, C. Folli, M. Stoppini, L. Olivi, A. Savoia, R. Berni, Structure of the trigonal crystal form of bovine annexin IV, Biochem. J. 329 (1998) 101–106.
[17] M.A. Kaetzel, Y.D. Mo, T.R. Mealy, B. Campos, W. Bergsma-Schutter, A. Brisson, J.R. Dedman, B.A. Seaton, Phosphorylation mutants elucidate the mechanism of annexin IV-mediated membrane aggregation, Biochemistry 40 (2001) 4192–4199.
[18] W.G. Hill, M.A. Kaetzel, B.K. Kishore, J.R. Dedman, M.L. Zeidel, Annexin A4 reduces water and proton permeability of model membranes but does not alter aquaporin 2-mediated water transport in isolated endosomes, J. Gen. Physiol. 121 (2003) 413–425.
[19] M.A. Kaetzel, H.C. Chan, W.P. Dubinsky, J.R. Dedman, D.J. Nelson, A role for annexin IV in epithelial cell function. Inhibition of calcium-activated chloride conductance, J. Biol. Chem. 269 (1994) 5297–5302.
[20] H. Sohma, C.E. Creutz, S. Gasa, H. Ohkawa, T. Akino, Y. Kuroki, Differential lipid specificities of the repeated domains of annexin IV, Biochim. Biophys. Acta 1546 (2001) 205–215.
[21] A. Piljic, C. Schultz, Annexin A4 self-association modulates general membrane protein mobility in living cells, Mol. Biol. Cell 17 (2006) 3318–3328.

Neuroscience Letters 534 (2013) 85–89

Contents lists available at SciVerse ScienceDirect

Neuroscience Letters

journal homepage: www.elsevier.com/locate/neulet

Proteomic analysis of the hippocampus in Alzheimer's disease model mice by using two-dimensional fluorescence difference in gel electrophoresis

Masaoki Takano[a], Takuya Yamashita[b,c], Kazuya Nagano[c], Mieko Otani[a], Kouji Maekura[a], Haruhiko Kamada[c], Shin-ichi Tsunoda[c], Yasuo Tsutsumi[b,c], Takami Tomiyama[e,f], Hiroshi Mori[e,f], Kenji Matsuura[d], Shogo Matsuyama[d,*]

[a] Laboratory of Molecular Cellular Biology, School of Pharmaceutical Sciences, Kobe Gakuin University, 1-1-3 Minatojima, Chuo-ku, Kobe 650-8586, Japan
[b] Laboratory of Toxicology and Safety Science, Graduate School of Pharmaceutical Sciences, Osaka University, 1-6 Yamadaoka, Suita, Osaka 565-0871, Japan
[c] Laboratory of Biopharmaceutical Research, National Institute of Biomedical Innovation, 7-6-8 Saito-Asagi, Ibaraki, Osaka 567-0085, Japan
[d] Faculty of Pharmaceutical Sciences, Himeji Dokkyo University, 7-2-1 Kamiohno, Himeji 670-8524, Japan
[e] Department of Neuroscience, Osaka City University Graduate School of Medicine, Osaka 545-8585, Japan
[f] Core Research for Evolutional Science and Technology, Japan Science and Technology Agency, Japan

HIGHLIGHTS

- We perform the proteome for $APP_{E693\Delta}$-transgenic mice. Methods are two-dimensional fluorescence difference in gel electrophoresis and mass spectrometry techniques. The expression of 14 proteins are changed in the brain. Aβ oligomers contribute to the expression of proteins.

ARTICLE INFO

Article history:
Received 4 August 2012
Received in revised form 13 October 2012
Accepted 6 November 2012

Keywords:
Proteome
Amyloid β oligomers
Alzheimer's disease
Hippocampus
2D-DIGE

ABSTRACT

We previously identified the E693Δ mutation in amyloid precursor protein (APP) in patients with Alzheimer's disease (AD) and then generated APP-transgenic mice expressing this mutation. As these mice possessed abundant Aβ oligomers from 8 months of age but no amyloid plaques even at 24 months of age, they are a good model to study pathological effects of amyloid β (Aβ) oligomers. The two-dimensional fluorescence difference in gel electrophoresis (2D-DIGE) technology, using a mixed-sample internal standard, is now recognized as an accurate method to determine and quantify proteins. In this study, we examined the proteins for which levels were altered in the hippocampus of 12-month-old $APP_{E693\Delta}$-transgenic mice using 2D-DIGE and liquid chromatography–tandem mass spectrometry (LC–MS/MS). Fourteen proteins were significantly changed in the hippocampus of $APP_{E693\Delta}$-transgenic mice. Actin cytoplasmic 1 (β-actin), heat shock cognate 71 kDa, γ-enolase, ATP synthase subunit β, tubulin β-2A chain, clathrin light chain B (clathrin) and dynamin-1 were increased. Heat shock-related 70 kDa protein 2, neurofilament light polypeptide (NFL), stress-induced-phosphoprotein 2, 60 kDa heat shock protein (HSP60), α-internexin, protein kinase C and casein kinase substrate in neurons protein 1 (Pacsin 1), α-enolase and β-actin were decreased. Western blotting also validated the changed levels of HSP60, NFL, clathrin and Pacsin 1 in $APP_{E693\Delta}$-transgenic mice. The identified proteins could be classified as cytoskeleton, chaperons, neurotransmission, energy supply and signal transduction. Thus, proteomics by 2D-DIGE and LC–MS/MS has provided knowledge of the levels of proteins in the early stages of AD brain.

1. Introduction

AD is neuropathologically characterized by abnormal accumulation of extracellular amyloid plaques and intracellular neurofibrillary tangles throughout cortical and limbic regions. Although the current amyloid cascade hypothesis [6] and tau hypothesis [15] provide frameworks for studying AD pathogenesis. Recently, diverse lines of evidence suggest that Aβ peptides play more important roles in AD pathogenesis [13,16,20]. Especially, soluble oligomers of Aβ could be a cause of synaptic and cognitive dysfunction in the early stages of AD. To address the relationship between Aβ oligomers and pathological features of AD, we generated APP transgenic mice expressing the E693Δ mutation, which enhanced Aβ oligomerization without fibrillization [25]. It might provide a clue for elucidating AD pathology caused by Aβ oligomers to analyze the $APP_{E693\Delta}$-transgenic mice.

* Corresponding author. Tel.: +81 79 223 6849; fax: +81 79 223 6857.
E-mail address: shogo@himeji-du.ac.jp (S. Matsuyama).

0304-3940/$ – see front matter © 2012 Elsevier Ireland Ltd. All rights reserved.
http://dx.doi.org/10.1016/j.neulet.2012.11.010

One of the most utilized approaches in proteomics to quantify and identify proteins is two dimensional gel electrophoresis (2DE) and mass spectrometry (MS) [5]. Proteomic approaches were most widely based on methods using differential expression on 2D-PAGE gels, or more recently 2D chromatography, followed by mass spectrometry protein identification. Compared to these conventional analyses, 2D-DIGE has higher reproducibility and sensitivity because of its internal standard design which minimizes gel-to-gel variation, improves spot matching, reduces number of gels needed, and permits quantitative analysis of small sample amounts.

In this study, we studied the altered expression of proteins in the hippocampus of $APP_{E693\Delta}$-transgenic mice using 2D-DIGE and LC–MS/MS approach. This approach revealed that the levels of at least 14 proteins were altered in the hippocampus of 12-month-old $APP_{E693\Delta}$-transgenic mice. These findings suggest that Aβ oligomers might cause synaptic and cognitive dysfunction by affecting the expression of these proteins in the hippocampus.

2. Experimental procedures

2.1. Materials

Sodium dodecyl sulfate, urea, thiourea, CHAPS, dithiothreitol, iodoacetamide, bromophenol blue, and RNase A and DNase I for SDS-PAGE or 2DE were all obtained from Wako Pure Chemical Industries (Osaka, Japan). Source information for all other assay reagents and materials are incorporated into their respective assay methods described below.

2.2. Animal subjects

Transgenic mice expressing human APP_{695} with the APP E693Δ mutation under the mouse prion promoter were used [25]. Heterozygous human $APP_{E693\Delta}$-transgenic mice and age-matched non-transgenic littermates were sacrificed at 12 months of age, and their hippocampi were isolated on an ice-cold plate. Animal care and handling were performed strictly in accordance with the Guidelines for Animal Experimentation at Kobe Gakuin University and Himeji Dokkyo University. Every effort was made to minimize the number of animals used and their suffering.

2.3. Protein labeling with CyDyes

Equal amounts of total protein from 4 hippocampi of $APP_{E693\Delta}$-transgenic mice or age-matched non-transgenic littermates were separately pooled. Protein samples were labeled with CyDyes (GE Healthcare, Piscataway, NJ), as per manufacturer's instructions. In brief, 50 μg of total protein from each sample was mixed in a tube and labeled with Cy2 minimal dye, and 50 μg protein taken from the mix was used as an internal standard on each gel for the three subsequent 2DE and image analysis. In parallel, 50 μg protein from each sample was labeled with either Cy3 or Cy5, and the dyes scrambled within each group to avoid possible dye bias. As a result, one replicate was Cy3 labeled proteins and another replicate was Cy5 labeled proteins. Two replicates (Cy3 and Cy5 labeled samples) were mixed, divided and applied each three independent gels. The sample volumes were adjusted to 18 μL with labeling buffer (7M urea, 2 M thiourea, 4% CHAPS, 30 mM Tris), followed by addition of 1 μL dye (working solution) to each individual sample. The samples were left on ice for 30 min in the dark, followed by adding 1 μL of 10 mmol/L lysine to stop the reaction.

2.4. 2D electrophoresis and image analysis

One sample from each of the CyDye groups was mixed together and adjusted to final concentrations of 1% DTT, 1% IPG buffer at a total volume of 350 μL with lysis buffer (7 M urea, 2 M thiourea, 4% CHAPS) and was used to 24 cm pH 4–7 IPG strips (non-linear; GE Healthcare, Piscataway, NJ) overnight. First dimension isoelectric focusing (IEF) was carried out with IPGphor II (GE Healthcare, Piscataway, NJ). Second dimension SDS-PAGE was performed by mounting the IPG strips onto 20 × 26 cm 12.5% DIGE gels (GE Healthcare, Piscataway, NJ) using Ettan DALT six Large Electrophoresis System (GE Healthcare, Piscataway, NJ) and running the gels at 16 mA/gel for the initial hour and 25 mA/gel at 25 °C constantly until bromophenol blue reached the bottom of the gel. The lysates were labeled at the ratio of 50 μg proteins: 400 pmol Cy3 or Cy5 protein-labeling dye (GE HealthcareBiosciences) in dimethylformamide according to the manufacturer's protocol.

In summary, three analytical gels were completed in total, running 25 μg of pooled reference sample labeled with Cy2, along with two samples (25 μg each), one labeled with Cy3 and the other labeled with Cy5. Gels selected for picking were stained with Deep purple (GE Healthcare, Piscataway, NJ). Approximately 1100 spots were matched across all three analytical gels. The analytical gel was picked using an automated robotic system, Ettan Spot picker (GE Healthcare, Piscataway, NJ). The pick list was created based on the Deep purple image. 2 mm gel plugs were picked, washed, reduced and alkylated, and then digested with trypsin, and the resulting peptides were extracted. Gel trypsinization was performed as previously described [24].

2.5. LC/MS/MS identification

Trypsinized peptides were analyzed by nano LC/MS/MS on a ThermoFisher LTQ Orbitrap XL. In brief, 30 mL of hydrolysate was loaded onto a 5 mm 675 mm ID C12 (Jupiter Proteo, Phenomenex) vented column at a flow-rate of 10 mL/min. Gradient elution was conducted on a 15 cm by 75 mm ID C12 column at 300 nL/min. A 30 min gradient was employed. The mass spectrometer was operated in a data-dependent mode, and the six most abundant ions were selected for MS/MS. Mass spectrometry results were searched using Mascot (www.matrixscience.com). Samples were processed in the Scaffold algorithm using DAT files generated by Mascot. Parameters for LTQ Orbitrap XL data require a minimum of two peptide matches per protein with minimum probabilities of 90% at the protein level.

2.6. Western blotting

Approximately 25 μg of protein from mouse hippocampus was applied to a 12.5% acrylamide gel and SDS-polyacrylamide gel electrophoresis was performed at 17.5 mA/gel for 2 h in second dimension. The gels were transferred onto PVDF membranes (Pall Corporation, Pensacola, FL, USA), in a trans-blot electrophoresis transfer cell (Nihon Eido, Tokyo, Japan). Western blotting was performed by using monoclonal antibodies against β-actin (diluted 1:1000, Cell Signaling, USA) and clathrin (diluted 1:250, Abcam, USA), polyclonal antibodies HSP60, NFL, voltage-dependent anion-selective channel protein 1 (VDAC) (diluted 1:1000, Cell Signaling, USA) and Pacsin 1 (diluted 1:500, Millipore, USA). Peroxidase-conjugated antibody (diluted 1:5000, Abcam, USA) was used as secondary antibody. The reaction was detected by chemiluminescence with ECL reagents (Pierce Biotechnology, USA). A semi quantitative analysis based on optical density was performed by ImageJ software (available at http://www.rsbweb.nih.gov/ij).

3. Results and discussion

The 2D-DIGE gels of the hippocampi from wild type and $APP_{E693\Delta}$-transgenic mice pools were shown as Fig. 1. Two replicates of each pooled sample were run, labeling one replicate with

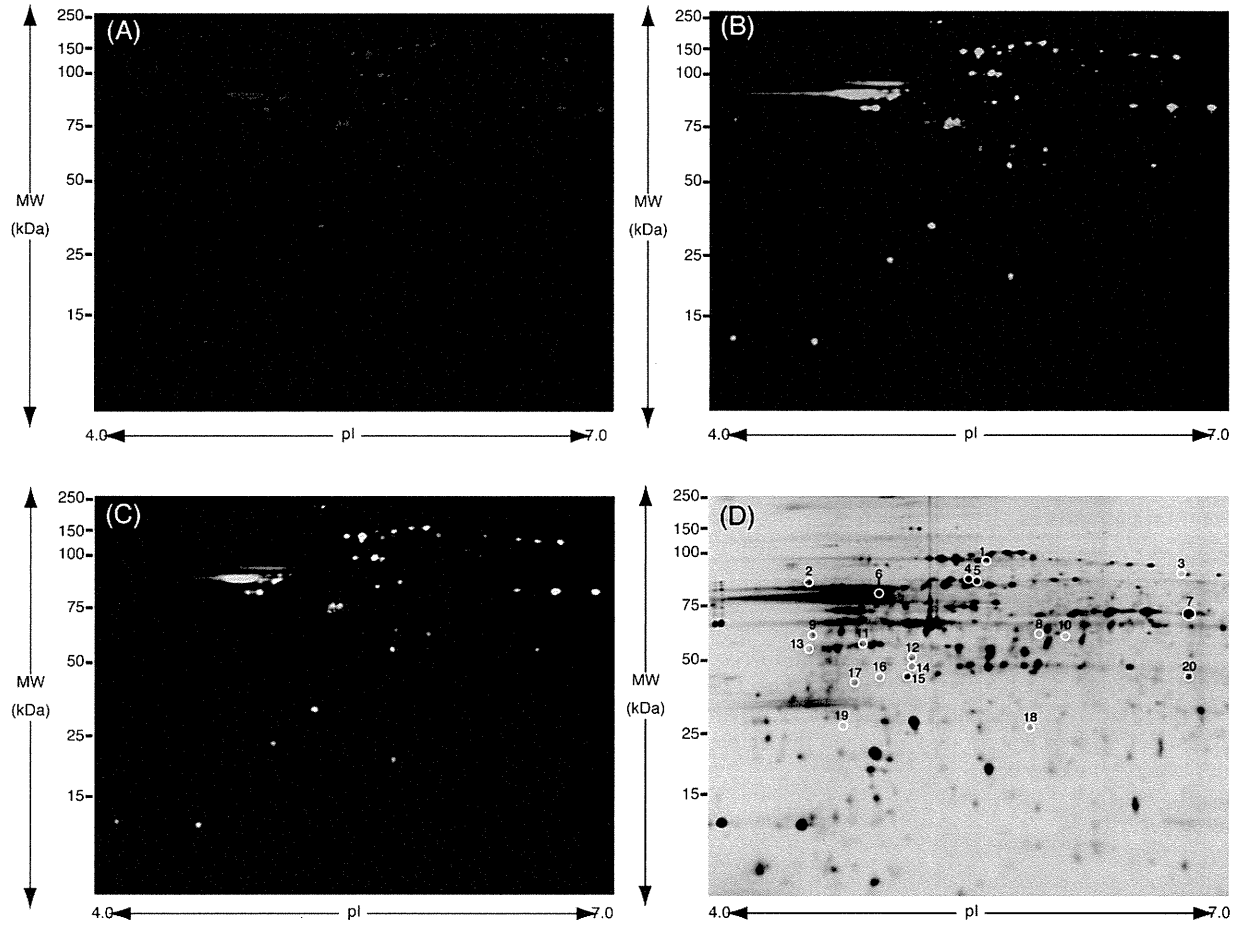

Fig. 1. 2D-DIGE gel image of fluorescence-labeled hippocampal proteins of non-transgenic and $APP_{E693\Delta}$-transgenic mice. (A) Analysis of the proteome of non-transgenic mice hippocampi with Cy3 Dye. (B) $APP_{E693\Delta}$-transgenic mice hippocampi with Cy5 Dye. (C) Merged. (D) Fourteen protein spots identified from non-transgenic and $APP_{E693\Delta}$-transgenic mice hippocampi by LC/MS/MS. Black numbers with white circles indicate proteins that are listed in Table 1.

Cy3 (Fig. 1A) and one replicate with Cy5 (Fig. 1B), resulting in three analytical gels. The 2D-DIGE comparative analysis of the wild type and $APP_{E693\Delta}$-transgenic mice revealed significant 74 spots (Fig. 1C). These spots were investigated by LC–MS/MS (Fig. 1D). Finally, fourteen proteins were identified as shown in Table 1. These proteins are classified into several groups that are involved in cytoskeletal, chaperone, energy metabolic, vesicle transport and signaling proteins (Table 2).

Spot nos. 1, 3 and 4 were identified as heat shock-related 70 kDa protein 2, stress-induced-phosphoprotein 1 and HSP60, respectively. The stress-induced-phosphoprotein 1 is the co-chaperone and thought of the function in regulation of interaction with Hsp70 and Hsp90 [10]. HSP60 is the chaperonin which is implicated in mitochondrial protein import and macromolecular assembly and may facilitate the correct folding of imported proteins [9]. The amounts of heat shock-related 70 kDa protein 2, stress-induced-phosphoprotein 1, and HSP60 were significantly decreased. On the contrary, spot no. 9 which was identified as heat shock cognate 71 kDa protein was significantly increased. This protein is also the chaperone and acts as a repressor of transcriptional activation [8]. Thus, Aβ oligomers might contribute to changing the expression of the chaperons.

Spot nos. 8, 10–12 and 16 were identified as actin, and spot nos. 15 and 17 were identified as tubulin β-2A chain. Actin is one of the major cytoskeletal proteins in neurons, and the dynamics of its assembly are involved in many aspects of cell motility, vesicle transport, and membrane turnover [14]. Actin itself is known to link with Aβ, which enhances the neurotoxicity induced by tau-mediated actin filament formation [4]. The four spots of actin but not no. 12 and those of tubulin were significantly increased. Thus, Aβ oligomers might lead to increasing the amounts of actin and tubulin.

Spot nos. 5 and 2 were identified as α-internexin and NFL, respectively, which are known as neuronal intermediate proteins [2,18]. The amounts of α-internexin and NFL were significantly decreased. Thus, the decreased amounts of NFL and internexin might raise neural dysfunction in the hippocampus of AD.

Spot nos. 7 and 13 were identified as α-enolase. Spot nos. 14 and 19 were identified as γ-enolase and ATP synthase subunit β, respectively. Enolase is a multifunctional protein as glycolytic enzyme, belonging to a novel class of surface proteins [11]. ATP synthase is a key role enzyme that provides energy for the cell to use through the synthesis of ATP [1]. The amount of α-enolase was significantly decreased, but the amounts of γ-enolase and ATP synthase subunit β were significantly increased. Interestingly, the levels of α-enolase and ATP synthase subunit α mitochondrial proteins significantly increased in the hippocampus of J20 Tg mice with amyloid deposition [19]. The amyloid deposit enhanced the expression of energy metabolic proteins [22]. Combined with our findings, both Aβ oligomers and amyloid deposition might play an important role in the change of energy metabolic proteins as α-enolase, γ-enolase and ATP synthase subunit β.

Spot no. 20 was identified as dynamin. Dynamin, a well studied neuron-specific mechanochemical GTPase, pinches off synaptic vesicles, freeing them from the membrane and allowing them to re-enter the synaptic vesicle pool to be refilled for future release

Table 1
Identified proteins from differentially expressed in the hippocampus of$APP_{E693\Delta}$-transgenic mice when compared to non-transgenic littermates.

Spot no.	Protein ID	Fold (APP/WT)	*t*-Test	Accession	Coverage	#Peptides	Predicted MW (kDa)	Calc. pI	Score
1	Heat shock-related 70 kDa protein 2	−1.32	0.040	P14659	26.22	23	69.6	5.67	625.70
2	Neurofilament light polypeptide	−1.48	0.002	P08551	39.96	43	61.5	4.64	1004.84
3	Stress-induced-phosphoprotein 1	−1.44	0.002	Q60864	16.21	9	62.5	6.80	157.49
4	60 kDa heat shock protein	−1.36	0.013	P63038	52.71	71	60.9	6.18	1916.39
5	Alpha-internexin	−1.34	0.023	P46660	42.66	39	55.7	5.27	1119.47
6	Protein kinase C and cascin kinase substrate in neurons protein 1	−1.48	0.023	Q61644	28.34	15	50.5	5.24	356.92
7	Alpha-enolase	−1.32	0.000	P17182	34.33	24	47.1	6.80	474.21
8	Actin, cytoplasmic 1	1.51	0.003	P60709	25.87	14	41.7	5.48	231.79
9	Heat shock cognate 71 kDa protein	1.35	0.015	P63017	12.54	16	70.8	5.52	319.85
10	Actin, cytoplasmic	1.34	0.004	P60709	24.27	13	41.7	5.48	279.37
11	Actin, cytoplasmic 1	1.38	0.022	P60709	15.47	7	41.7	5.48	243.14
12	Actin, cytoplasmic 1	−1.56	0.013	P60709	22.67	12	41.7	5.48	131.57
13	Gamma-enolase	1.33	0.005	P17183	20.05	13	47.3	5.11	237.25
14	ATP synthase subunit beta	1.40	0.047	P56480	23.60	18	56.3	5.34	356.19
15	Tubulin beta-2A chain	1.31	0.021	Q13885	14.83	13	49.9	4.89	313.07
16	Actin, cytoplasmic 1	1.47	0.002	P60709	6.93	3	41.7	5.48	97.01
17	Tubulin beta-2S chain	1.44	0.009	Q13885	11.46	5	49.9	4.89	118.50
18	Clathrin light chain B	1.68	0.005	P09497	8.30	3	25.2	4.64	95.06
19	ATP synthase subunit beta	1.46	0.013	P06576	16.64	16	56.5	5.40	283.06
20	Dynamin-1	1.40	0.006	Q05193	9.61	13	97.3	7.17	242.16

Mass spectrometry protein identification of 2D-DIGE spots of interest and statistical analysis using *t*-test between wild type mice and $APP_{E693\Delta}$-transgenic mice gels ($P < 0.05$). The proteins of mouse hippocampus were separated by 2DE and identified by LC MS/MS, following in-gel digestion with trypsin. The spots representing identified proteins are indicated in Fig. 1D and are designated with their ID accession numbers of Swiss Prot database. Score relates to the probability assignment. Score and sequence coverage were calculated by MASCOT search engine (http://www.matrixscience.com).

Table 2
Functions regulated by proteins that showed an altered expression in $APPE_{693\Delta}$-transgenic mouse hippocampus.

Function	Identified protein	Up/down
Cytoskeletal and their interacting proteins	Neurofilament light polypeptide	Down
	Alpha-internexin	Down
	Actin, cytoplasmic 1	Up/down
	Tubulin β-2A Chain	Up
Chaperone and their interacting proteins	Stress-induced-phosphoprotein 1	Down
	60 kDa heat shock protein	Down
	Heat shock cognate 71 kDa protein	Down
Energy metabolic proteins	Alpha-enolase	Down
	Gamma-enolase	Up
	ATP synthase subunit beta	Up
Vesicle transport and recycling	Dynamin-1	Up
	Clathrin light chain B	Up
Signaling proteins	Protein kinase C and casein kinase substrate in neurons protein 1	Down

The analysis of proteins function was done by using MOTIF (http://www.genome.jp/tools/motif/).

[12]. The amount of dynamin was significantly increased. Our findings in $APP_{E693\Delta}$-transgenic mice without plaque deposition are consistent with previous findings that protein levels of dynamin were increased in Tg2576 mice with plaque deposition [21], suggesting that the release of neurotransmitter is affected by dynamin increased irrespective of AD stage. Also, spot no. 6 was identified as Pacsin 1. The Pacsin 1 is colocalized, oligomerized and bound with dynamin, and both proteins participate in synaptic vesicle endocytosis [17]. The amount of Pacsin 1 was significantly increased. Taken together, Pacsin 1 and dynamin enhanced by Aβ oligomers

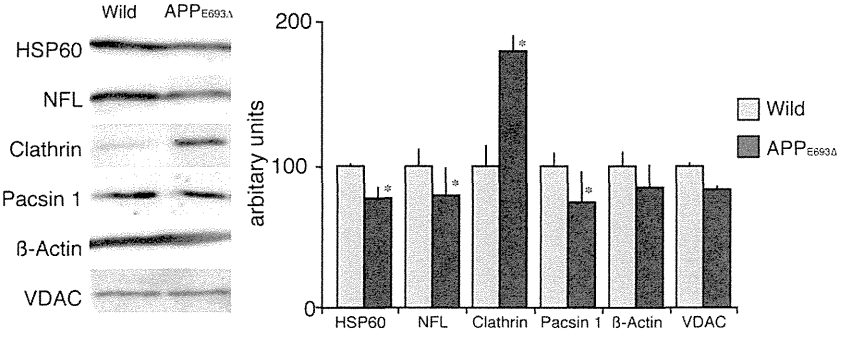

Fig. 2. Differentially expressed proteins validated by Western blotting for the hippocampus of non-transgenic and $APP_{E693\Delta}$-transgenic mice. (A) The levels of HSP60, NFL, clathrin, Pacsin 1, β-actin and VDAC in individual samples of each group were detected. (B) Graphical representation of the semi quantitative analysis (mean ± SEM of O.D. of bands). Data are presented as mean ± SEM ($n = 4$) *t*-test; $^*P < 0.05$ vs. $APP_{E693\Delta}$-transgenic mice.

might change the function of synaptic vesicle in the hippocampus of AD.

Spot no. 18 was identified as clathrin, which is known as the major protein of the polyhedral coat of coated pits and vesicles [7]. The amount of spot no. 18 was significantly decreased. APP was associated clusters of clathrin-coated vesicles and endosomes [3]. Thus, Aβ oligomers might inhibit the vesicle formation by clathrin.

In addition, we performed a validation experiment for HSP60, NFL, clathrin, Pacsin 1 and β-actin as the altered proteins, and VDAC as the unchanged protein (as control) [23]. The increased levels of clathrin, the decreased levels of HSP60, NFL, and Pacsin 1 and the unchanged level of β-actin and VDAC in $APP_{E693\Delta}$-transgenic mice hippocampus were validated by Western blotting (Fig. 2).

In summary, we identified the altered levels of 14 proteins in $APP_{E693\Delta}$-transgenic mice hippocampus using 2D-DIGE and LC–MS/MS approach. This approach elucidated the pathological effects of Aβ oligomers on hippocampus. Our findings might provide a clue for investigation of the hippocampus of AD early stage.

Acknowledgements

This work was supported by grants from Kobe Gakuin University for Collaborative Research C and the Smoking Research Foundation. The authors thank Dr. Tadanori Mayumi for his encouragement during the early days of the study.

References

[1] U. Andersson, H. Antonicka, J. Houstek, B. Cannon, A novel principle for conferring selectivity to poly(A)-binding proteins: interdependence of two ATP synthase beta-subunit mRNA-binding proteins, Biochemical Journal 346 (Pt 1) (2000) 33–39.
[2] C.L. Chien, R.K. Liem, Characterization of the mouse gene encoding the neuronal intermediate filament protein alpha-internexin, Gene 149 (1994) 289–292.
[3] A. Ferreira, A. Caceres, K.S. Kosik, Intraneuronal compartments of the amyloid precursor protein, Journal of Neuroscience 13 (1993) 3112–3123.
[4] T.A. Fulga, I. Elson-Schwab, V. Khurana, M.L. Steinhilb, T.L. Spires, B.T. Hyman, M.B. Feany, Abnormal bundling and accumulation of F-actin mediates tau-induced neuronal degeneration in vivo, Nature Cell Biology 9 (2007) 139–148.
[5] A. Gorg, C. Obermaier, G. Boguth, A. Harder, B. Scheibe, R. Wildgruber, W. Weiss, The current state of two-dimensional electrophoresis with immobilized pH gradients, Electrophoresis 21 (2000) 1037–1053.
[6] J. Hardy, D.J. Selkoe, The amyloid hypothesis of Alzheimer's disease: progress and problems on the road to therapeutics, Science 297 (2002) 353–356.
[7] J. Hirst, M.S. Robinson, Clathrin and adaptors, Biochimica et Biophysica Acta 1404 (1998) 173–193.
[8] C.R. Hunt, A.J. Parsian, P.C. Goswami, C.A. Kozak, Characterization and expression of the mouse Hsc70 gene, Biochimica et Biophysica Acta 1444 (1999) 315–325.
[9] S. Ikawa, R.A. Weinberg, An interaction between p21ras and heat shock protein hsp60, a chaperonin, Proceedings of the National Academy of Sciences 89 (1992) 2012–2016.
[10] J.L. Johnson, A. Halas, G. Flom, Nucleotide-dependent interaction of Saccharomyces cerevisiae Hsp90 with the cochaperone proteins Sti1, Cpr6, and Sba1, Molecular and Cellular Biology 27 (2007) 768–776.
[11] M. Kaghad, X. Dumont, P. Chalon, J.M. Lelias, N. Lamande, M. Lucas, M. Lazar, D. Caput, Nucleotide sequences of cDNAs alpha and gamma enolase mRNAs from mouse brain, Nucleic Acids Research 18 (1990) 3638.
[12] B.L. Kelly, R. Vassar, A. Ferreira, Beta-amyloid-induced dynamin 1 depletion in hippocampal neurons. A potential mechanism for early cognitive decline in Alzheimer disease, Journal of Biological Chemistry 280 (2005) 31746–31753.
[13] W.L. Klein, G.A. Krafft, C.E. Finch, Targeting small Abeta oligomers: the solution to an Alzheimer's disease conundrum? Trends in Neurosciences 24 (2001) 219–224.
[14] T.B. Kuhn, P.J. Meberg, M.D. Brown, B.W. Bernstein, L.S. Minamide, J.R. Jensen, K. Okada, E.A. Soda, J.R. Bamburg, Regulating actin dynamics in neuronal growth cones by ADF/cofilin and rho family GTPases, Journal of Neurobiology 44 (2000) 126–144.
[15] V.M. Lee, M. Goedert, J.Q. Trojanowski, Neurodegenerative tauopathies, Annual Review of Neuroscience 24 (2001) 1121–1159.
[16] S. Li, S. Hong, N.E. Shepardson, D.M. Walsh, G.M. Shankar, D. Selkoe, Soluble oligomers of amyloid Beta protein facilitate hippocampal long-term depression by disrupting neuronal glutamate uptake, Neuron 62 (2009) 788–801.
[17] J. Modregger, B. Ritter, B. Witter, M. Paulsson, M. Plomann, All three PACSIN isoforms bind to endocytic proteins and inhibit endocytosis, Journal of Cell Science 113 (Pt 24) (2000) 4511–4521.
[18] R.A. Nixon, R.K. Sihag, Neurofilament phosphorylation: a new look at regulation and function, Trends in Neurosciences 14 (1991) 501–506.
[19] R.A. Robinson, M.B. Lange, R. Sultana, V. Galvan, J. Fombonne, O. Gorostiza, J. Zhang, G. Warrier, J. Cai, W.M. Pierce, D.E. Bredesen, D.A. Butterfield, Differential expression and redox proteomics analyses of an Alzheimer disease transgenic mouse model: effects of the amyloid-beta peptide of amyloid precursor protein, Neuroscience 177 (2011) 207–222.
[20] D.J. Selkoe, Alzheimer's disease is a synaptic failure, Science 298 (2002) 789–791.
[21] S.J. Shin, S.E. Lee, J.H. Boo, M. Kim, Y.D. Yoon, S.I. Kim, I. Mook-Jung, Profiling proteins related to amyloid deposited brain of Tg2576 mice, Proteomics 4 (2004) 3359–3368.
[22] R. Sultana, D. Boyd-Kimball, J. Cai, W.M. Pierce, J.B. Klein, M. Merchant, D.A. Butterfield, Proteomics analysis of the Alzheimer's disease hippocampal proteome, Journal of Alzheimer's Disease 11 (2007) 153–164.
[23] M. Takano, K. Maekura, M. Otani, K. Sano, T. Nakamura-Hirota, S. Tokuyama, K.S. Min, T. Tomiyama, H. Mori, S. Matsuyama, Proteomic analysis of the brain tissues from a transgenic mouse model of amyloid beta oligomers, Neurochemistry International 61 (2012) 347–355.
[24] M. Takano, M. Otani, A. Sakai, K. Kadoyama, S. Matsuyama, A. Matsumoto, M. Takenokuchi, M. Sumida, T. Taniguchi, Use of a phosphosensor dye in proteomic analysis of human mutant tau transgenic mice, Neuroreport 20 (2009) 1648–1653.
[25] T. Tomiyama, S. Matsuyama, H. Iso, T. Umeda, H. Takuma, K. Ohnishi, K. Ishibashi, R. Teraoka, N. Sakama, T. Yamashita, K. Nishitsuji, K. Ito, H. Shimada, M.P. Lambert, W.L. Klein, H. Mori, A mouse model of amyloid beta oligomers: their contribution to synaptic alteration, abnormal tau phosphorylation, glial activation, and neuronal loss in vivo, Journal of Neuroscience 30 (2010) 4845–4856.

—Review—

抗体工学を駆使した創薬ターゲットの探索技術

鎌田春彦

Exploring Technique for Pharmaceutical Target Using Antibody Technology

Haruhiko Kamada

Laboratory of Biopharmaceutical Research, National Institute of Biomedical Innovation; 7-6-8 Saito-Asagi, Ibaraki, Osaka 567-0085, Japan.

(Received December 2, 2011)

A monoclonal antibody (Mab), due to its specific binding ability to a target protein, can potentially be one of the most useful tools for the functional analysis of proteins in recent proteomics-based research. However, the production of Mab is a very time-consuming and laborious process (*i.e.*, preparation of recombinant antigens, immunization of animals, preparation of hybridomas), making it the rate-limiting step in using Mabs in high-throughput proteomics research, which heavily relies on comprehensive and rapid methods. Therefore, there is a great demand for new methods to efficiently generate Mabs against a group of proteins identified by proteome analysis. Here, we describe a useful method called "Antibody proteomic technique" for the rapid generations of Mabs to pharmaceutical target, which were identified by proteomic analyses of disease samples (ex. tumor tissue, *etc.*). We also introduce another method to find profitable targets on vasculature, which is called "Vascular proteomic technique". Our results suggest that this method for the rapid generation of Mabs to proteins may be very useful in proteomics-based research as well as in clinical applications.

Key words——monoclonal antibody; proteomics; biomarker; biologics

1. はじめに

近年，ゲノム解析やジーンチップ解析などのオミクス研究の進展に伴い，バイオマーカー探索や創薬のための標的分子の探索が盛んに行われている．[1,2] このような医薬品開発に資する標的分子の探索は，画期的な医薬品を開発する上で最も重要なステップであり，探索の結果から得られた標的分子に作用する薬物は，これまで治療法のなかった疾患の治療に貢献すると考えられている．このような疾患の発症や悪化の原因となる標的分子の探索のうち，とりわけプロテオミクスを用いたタンパク質の発現解析は注目を集めており，医薬品の開発に貢献するものと期待されている．[3] しかしながら，上述したオミクス解析全般に言えることであるが，標的分子の探索から創薬ターゲットの発見につながった例はこれまでほとんどないのが現状である．疾患の発症や悪化に連動して発現変化が認められる疾患関連分子は，病態時に数百以上のオーダーで発現変動しており，そのほとんどが疾患の発症や悪化には直接関係していないものであるとされている．[4] したがって，画期的診断法・治療法を開発していくためには，このような疾患関連分子の中から，創薬に資する分子を効率よく同定する必要があり，これまで用いられてきた方法をより進歩させた新しい探索法の開発に期待が寄せられている．

このように標的分子を検出したり薬理効果発現を評価したりするためには，標的分子を認識可能なプローブが必要であり，標的分子候補タンパク質に結合活性を持つ抗体の開発がますます重要視されつつある．特に，最近では抗体そのものを医薬品化した抗体医薬品がリウマチやがんなど様々な難治性疾患に臨床応用され，バイオ医薬品の市場規模が急拡大している．[5] これまでに臨床応用された抗体医薬品としては抗サイトカイン抗体などの活性中和抗体や細胞表面のマーカー分子を認識する抗細胞抗体がほ

独立行政法人医薬基盤研究所バイオ創薬プロジェクト（〒567-0085 大阪府茨木市彩都あさぎ7-6-8）
e-mail: kamada@nibio.go.jp

本総説は，日本薬学会第131年会シンポジウムS16で発表したものを中心に記述したものである．

とんどであるが，最近では受容体に結合して活性を示すアゴニスト抗体や2種類のマーカー分子を認識して活性を示すバイスペシフィック抗体なども臨床応用に向けた検討が進められつつある.[6]

このような抗体医薬は，従来の低分子医薬品や分子プローブでは困難な疾患に対する治療や診断が可能であるために，様々な難治性疾患の克服に向け大いに利用されつつあるところであるが，抗体医薬の開発を効率よく進めるためにはいくつかの問題点があることが知られている．その1つの問題点として，一般的に1種類の抗体の作製期間は，数ヵ月程度必要とされ，このことが原因となって標的分子が同定されてからその評価までには大きなタイムラグが生じており，タンパク質の中からスクリーニングする上での障害となっていることが指摘されている.

もし数多くの発現変動タンパク質に対する特異的抗体が一挙かつ迅速に作製できれば，定量解析（ELISA, Western blot (WB), *etc.*），局在解析（免疫染色，WB, *etc.*），機能解析（細胞増殖活性，細胞分化解析，*etc.*）が可能になり，タンパク質の発現挙動と疾患の発症・悪化などとの連関解析が格段に進展するものと考えられる．そこでわれわれは，プロテオーム解析技術の最適化とともに，数多くの変動タンパク質の中から，創薬に向けて標的分子を絞り込む基盤技術の開発を行うために，プロテオミクスと抗体工学を融合させた新しい「抗体プロテオミクス技術」を開発した．本総説では，この「抗体プロテオミクス技術」を概説し創薬ターゲット候補分子の同定に至った例を示すとともに，抗体をバイオ医薬品として利用する際に有用な探索技術として「血管プロテオミクス」に関してもその研究成果を一部紹介する.

2. 抗体プロオミクス技術

抗体は生体内で外来異物由来のタンパク質抗原を認識し，それを捕捉するための生体防御分子としての役割を持っている．すなわち，あらゆる外来抗原に対して，結合可能なレパートリーを有するタンパク分子群である．その性質を利用し，古くからタンパク質の定性や定量のためのツールとして，生命科学の分野で活用されている．われわれは，この抗体の持つ性質に着目し，生体の抗体レパートリーを再現した抗体ライブラリを手に持つことで，抗原に結合可能な抗体分子を短時間で手に入れたいと考えた．この膨大な抗体ライブラリの中から目的の抗体を迅速に単離するための基盤技術としてわれわれはファージ抗体ライブラリに着目した．このファージ抗体ライブラリは，抗体の抗原認識部位にあたるV領域をリンカーで結んだ一本鎖抗体（scFV 抗体）をファージの外殻タンパク質gⅢとの融合タンパク質としてファージ表面に提示しており，ファージウイルスの表面に提示させた一本鎖抗体をライブラリとして作製することが可能である.[7] この技術は，一般的に用いられるハイブリドーマ法とは異なり，*in vitro* のセレクションのみで迅速にモノクローナル抗体を単離することができ，2週間程度の短期間でモノクローナル抗体が得られる方法である．この技術を従来から知られる二次元電気泳動法などを利用したプロテオミクス技術と組み合わせ，単離・精製したタンパク質に対して上述した抗体ライブラリからの抗体の単離を行おうと考えた．さらに得られた抗体を利用し，免疫染色を利用した抗原の発現解析を組織マイクロアレイを用いて迅速に行うことにした．この組織マイクロアレイは，がんなどの疾患組織が直径1–2 mm程度の組織片として添付されたスライドガラスであり，一挙に100症例以上もの組織を免疫染色などで検出することが可能である.[8] この組織マイクロアレイを用いることで，これまで発現解析が困難であった組織を一挙に染色でき，極めて短時間にタンパク質の発現状態を知ることができる．この抗体ライブラリをプロテオミクス，さらに組織マイクロアレイと融合した「抗体プロテオミクス技術」をわれわれは独自に開発し，がんの標的分子の探索を行うことにした（Fig. 1）.[9]

まず，ナイーブファージ抗体ライブラリをウェスタンブロット等に用いられるメンブランに固相化した精製タンパク質に対してパンニングを行い，わずか10 ng程度のモデル抗原からでもモノクローナル抗体を得ることができた．さらに，この方法を乳がんの診断・治療に応用し，画期的な標的分子の探索を行うために，正常乳腺とのタンパク質比較解析を行った．その結果，十数種類前後の標的分子候補の中から最も有用な創薬ターゲットとしてEphrin Receptor A10（EphA10）と呼ばれる分子を同定した（Table 1）．この分子は，乳がん細胞に特異的に発現する上，既存の乳がんの標的分子として知られるHer-2よりも高い陽性率を示し，Her-2陰性患者

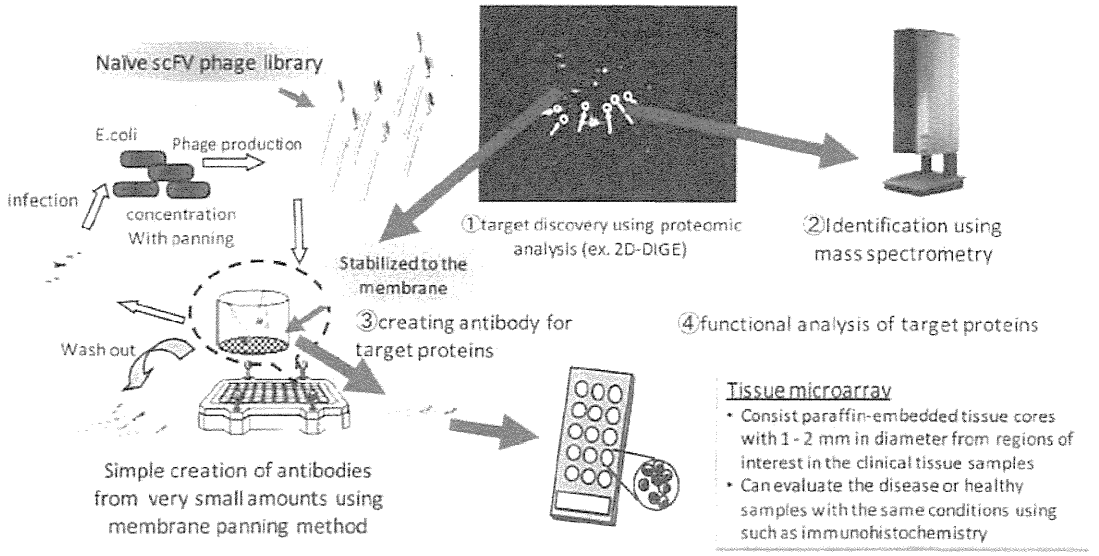

Fig. 1. Schematic Protocol of Antibody Proteomics

Table 1. Protein Expression of Identified Drug Target Candidates Using Tissue Microarray

Target candidate	Positive ratio	
	Healthy mammal	Breast cancer
Her2 (Control)	0/15(0%)	53/189(28%)
IkappaBR	3/15(20%)	22/189(12%)
SPATA5 protein	0/15(0%)	0/189(0%)
beta actin variant	0/15(0%)	0/189(0%)
TRAIL-R2	0/15(0%)	119/189(63%)
RREB-1	1/15(6%)	83/189(44%)
FLJ31438 protein	0/15(0%)	0/189(0%)
hPAK65	0/15(0%)	0/189(0%)
Cytokeratin 8	0/15(0%)	137/189(73%)
XRN1 protein	0/15(0%)	0/189(0%)
Jerky protein homolog-like	0/15(0%)	0/189(0%)
EPH receptor A10 (EphA10)	0/15(0%)	93/189(49%)

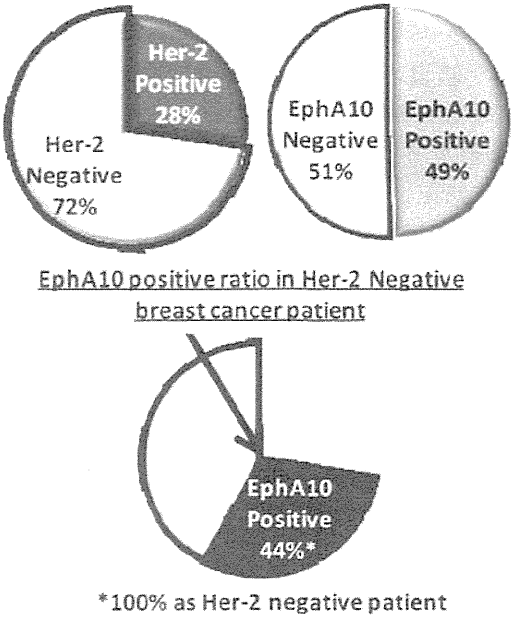

Fig. 2. EphA10 Expression in Breast Cancer Patients

の約半数に発現する創薬ターゲットとしても有用性の高い分子であることが明らかになった（Fig. 2）.

3. 血管プロテオミクス

このように創薬ターゲットとしての分子探索にプロテオミクスの手法を用いることは極めて有用であり，今後数多くの標的分子を発見できる可能性を示唆している．その一方で，現在の抗体医薬の標的分子のほとんどが，膜タンパク質及び分泌タンパク質を標的とした分子標的治療薬である事実からも，抗体医薬を用いる限り，現在の技術背景では，細胞質内に存在するタンパク質を標的にするのは数多くの問題点があると考えられている．[10] したがって，抗体医薬の開発を念頭に置く場合には，膜タンパク質や分泌タンパク質を標的にすることが実用化において最も近道であると考えられる．そこで，細胞膜タンパク質，及び細胞外マトリクス等の分泌タンパク質の発現挙動の解析のために，全身の血管をビオチン化試薬にてラベル化し，疾患組織にある血管内皮

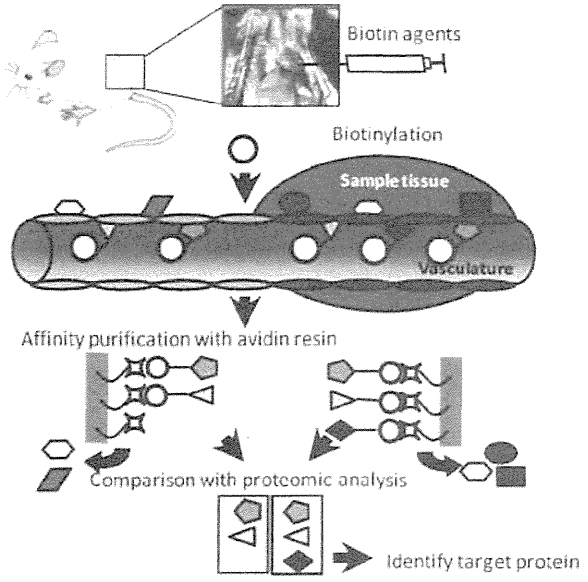

Fig. 3. Schematic Protocol of Vasculature Proteomics

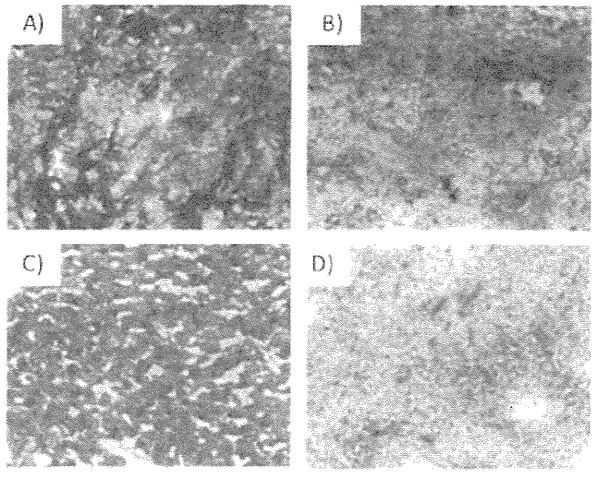

Fig. 4. BST-2 Expression in Metastatic Lymphoma

(A) Liver metastatic tumor; (B) Spleen metastatic tumor; (C) Normal liver; (D) Normal spleen. Immunohistochemistry were performed by using anti-BST-2 polyclonal antibody. Tumor vascular regions were stained (dark gray) but not normal tissues.

細胞の膜タンパク質並びに分泌タンパク質を効率よく回収・精製可能な *in vivo* biotinylation 法を活用し血管プロテオームを行うことにした.[11] Figure 3 にその概要を示す. この *in vivo* biotinylation 法は, 細胞膜タンパク質を解析する場合に, 現在汎用されている組織抽出後の膜タンパク質を回収する方法とは異なり, 直接組織細胞の外側からラベル化を行うため, 小胞膜のコンタミネーションのリスクを回避できる. 当然のことながら, 細胞外の膜タンパク質等を選択的にビオチンラベルするため, 解析結果から得られたタンパク質候補に対するモノクローナル抗体は, 通常の方法でプロテオーム解析して得られたタンパク質候補（多くの場合, シャペロンタンパク質やヒートショックタンパク質といった細胞内タンパク質）に対する抗体よりも, 基礎医学・臨床医学的な有用性に優れていることは言うまでもない. そのうえ, 血管側からビオチン化しているため, 組織中の血管内皮細胞がより効率よくラベル化されており, 抗体医薬の開発には極めて有用な方法であると考えられる.

この血管プロテオミクスを担がんマウスモデルに対して行い, 転移性リンパ腫の治療に向けた抗原の探索を行った.[12] 具体的には, 抗体のラベル化等に用いるビオチン化試薬を, *in vivo* に直接投与・環流することで, 組織に存在する血管を直接ラベル化した. その結果, 腫瘍血管での発現がこれまでにも報告されている Transferrin 受容体が同定された一方, これまで知られていなかった新しいがん血管関連抗原として BST-2 の発現を見い出した（Fig. 4）.[12] BST-2 は, 肝臓や脾臓に転移したリンパ腫の血管部位に特異的に発現しており, これを標的としたがん治療薬の開発が期待される. 実際に, この BST-2 に対する抗体を投与することで, 腫瘍の増殖が抑制される結果も見い出しており, 今後これらを利用した抗体医薬の開発も期待されるところである.

4. 結論と展望

抗体プロテオミクス技術はプロテオミクスと抗体工学の技術を組み合わせ, さらに組織マイクロアレイによるバリデーションを迅速に行うことで, 標的分子を迅速にバリデーションできる技術である. この技術により, これまで標的分子の探索から発現解析までの膨大な時間と労力を, わずか 2–3 週間程度の期間で達成できる極めて有用な技術として開発することができた. また先述したように血管プロテオミクスは, 個体レベルでのプロテオミクスを可能とするうえ, 細胞膜タンパク質及び細胞外マトリクス等の分泌タンパク質を効果的にラベル化できる方法であり, 細胞質内タンパク質のコンタミネーションを回避できるという圧倒的な利点を有している. この 2 つのプロテオミクス技術を融合することで, 疾患における創薬ターゲットの同定に留まらず, 新しい抗体医薬の開発法として利用することを考えてい

る．今後，本方法を用いて同定された抗原に対する抗体を作製することで，バイオマーカーの検出や評価に利用できるものと期待されるとともに，タンパク質の発現挙動解析，並びに同定作業を現在も進めているところであり，プロテオミクスによる解析基盤の確立に向けた開発・最適化を今後も行う予定である．

謝辞　本研究は，多くの共同研究者の先生方に御支援を賜りつつ，大阪大学薬学研究科毒性学分野及び医薬基盤研究所バイオ創薬プロジェクトのスタッフ・学生の皆さんとともに推進したものです．この場をお借りして，心より御礼を申し上げます．さらに，プロテオーム解析にあたり医薬基盤研究所免疫シグナルプロジェクト 世良田 聡先生，伸 哲治先生にご協力頂くとともに，血管プロテオミクスに関しては，スイス連邦工科大学チューリッヒ校(ETHZ)のダリオ・ネリ教授のご協力を得ました．また本研究の推進にあたり，厚生労働科学研究費補助金並びに文部科学研究費補助金の支援を賜りました．ここに深謝申し上げます．

REFERENCES

1) Kramer R., Cohen D., *Nat. Rev. Drug Discov.*, **3**, 965–972 (2004).
2) Butte A., *Nat. Rev. Drug Discov.*, **1**, 951–960 (2002).
3) Latterich M., Schnitzer J. E., *Nat. Biotechnol.*, **29**, 600–602 (2011).
4) Rifai N., Gillette M. A., Carr S. A., *Nat. Biotechnol.*, **24**, 971–983 (2006).
5) Goodman M., *Nat. Rev. Drug Discov.*, **8**, 837 (2009).
6) Nelson A. L., Reichert J. M., *Nat. Biotechnol.*, **27**, 331–337 (2009).
7) Yamashita T., Utoguchi N., Suzuki R., Nagano K., Tsunoda S., Tsutsumi Y., Maruyama K., *Yakugaku Zasshi*, **130**, 479–485 (2010).
8) Giltnane J. M., Rimm D. L., *Nat. Clin. Pract. Oncol.*, **1**, 104–111 (2004).
9) Imai S., Nagano K., Yoshida Y., Okamura T., Yamashita T., Abe Y., Yoshikawa T., Yoshioka Y., Kamada H., Mukai Y., Nakagawa S., Tsutsumi Y., Tsunoda S., *Biomaterials*, **32**, 162–169 (2011).
10) Williams B. R., Zhu Z., *Curr. Med. Chem.*, **13**, 1473–1480 (2006).
11) Roesli C., Neri D., *J. Proteomics*, **73**, 2219–2229 (2010).
12) Schliemann C., Roesli C., Kamada H., Borgia B., Fugmann T., Klapper W., Neri D., *Blood*, **115**, 736–744 (2010).

IJC
International Journal of Cancer

CD34$^+$/CD38$^-$ acute myelogenous leukemia cells aberrantly express CD82 which regulates adhesion and survival of leukemia stem cells

Chie Nishioka[1,2], Takayuki Ikezoe[3], Mutsuo Furihata[4], Jing Yang[3], Satoshi Serada[5], Tetsuji Naka[5], Atsuya Nobumoto[6], Sayo Kataoka[7], Masayuki Tsuda[6], Keiko Udaka[1] and Akihito Yokoyama[3]

[1] Department of Immunology, Kochi Medical School, Kochi University, Nankoku, Kochi, Japan
[2] Japanese Society for the Promotion of Science (JSPS), Chiyoda-ku, Tokyo, Japan
[3] Hematology and Respiratory Medicine, Kochi Medical School, Kochi University, Nankoku, Kochi, Japan
[4] Tumor Pathology, Kochi Medical School, Kochi University, Nankoku, Kochi, Japan
[5] Laboratory for immune Signal, National Institute of Biomedical Innovation, Ibaraki, Osaka
[6] The Facility for Animal Research, Kochi Medical School, Kochi University, Nankoku, Kochi, Japan
[7] Medical Research Center, Kochi Medical School, Kochi University, Nankoku, Kochi, Japan

To identify molecular targets in leukemia stem cells (LSCs), this study compared the protein expression profile of freshly isolated CD34$^+$/CD38$^-$ cells with that of CD34$^+$/CD38$^+$ counterparts from individuals with acute myelogenous leukemia (n = 2, AML) using isobaric tags for relative and absolute quantitation (iTRAQ). A total of 98 proteins were overexpressed, while six proteins were underexpressed in CD34$^+$/CD38$^-$ AML cells compared with their CD34$^+$/CD38$^+$ counterparts. Proteins overexpressed in CD34$^+$/CD38$^-$ AML cells included a number of proteins involved in DNA repair, cell cycle arrest, gland differentiation, antiapoptosis, adhesion, and drug resistance. Aberrant expression of CD82, a family of adhesion molecules, in CD34$^+$/CD38$^-$ AML cells was noted in additional clinical samples (n = 12) by flow cytometry. Importantly, down-regulation of CD82 in CD34$^+$/CD38$^-$ AML cells by a short hairpin RNA (shRNA) inhibited adhesion to fibronectin *via* up-regulation of matrix metalloproteinases 9 (MMP9) and colony forming ability of these cells as assessed by transwell assay, real-time RT-PCR, and colony forming assay, respectively. Moreover, we found that down-regulation of CD82 in CD34$^+$/CD38$^-$ AML cells by an shRNA significantly impaired engraftment of these cells in severely immunocompromised mice. Taken together, aberrant expression of CD82 might play a role in adhesion of LSCs to bone marrow microenvironment and survival of LSCs. CD82 could be an attractive molecular target to eradicate LSCs.

Key words: AML, leukemia stem cells, bone marrow microenvironment, CD82, MMP9
Additional Supporting Information may be found in the online version of this article.
*Takayuki Ikezoe contributed to the concept and design, interpreted and analyzed the data and wrote an article. Chie Nishioka performed all experiments and wrote an article. Mutsuo Furihata, Jing Yang, Satoshi Serada, and Tetsuji Naka, Sayo Kataoka and Atsuya Nobumoto performed the experiments. Akihito Yokoyama and Keiko Udaka provided important intellectual content
Grant sponsors: The Kochi University President's Discretionary Grant, Setsuro Fujii Memorial, The Osaka Foundation for Promotion of Fundamental Medical Research, Certificate of Kochi Shin-kin/Anshin-tomo-no-kai Prize and Japan Society for the Promotion of Science
DOI: 10.1002/ijc.27904
History: Received 15 Mar 2012; Accepted 25 Sep 2012; Online 11 Oct 2012
Correspondence to: Takayuki Ikezoe, Department of Hematology and Respiratory Medicine, Kochi University, Oko-cho, Nankoku, Kochi 783-8505, Japan, Tel.: 81-88-880-2345, Fax: 81-88-880-2348, E-mail: ikezoet@kochi-u.ac.jp

Acute myelogenous leukemia (AML) is characterized by a cellular hierarchy, and is initiated and maintained by a subset of self-renewing leukemia stem cells (LSCs).[1] To produce cure in individuals with AML, development of a novel treatment strategy targeting LSCs is urgently required. LSCs share some antigenic features with normal hematopoietic stem cells (HSCs). For example, both LSCs and HSCs express CD34 but not CD38. However, LSCs can be phenotypically distinguished from HSCs by several disparate markers, including CD117$^-$ and CD123$^+$.[1–3] LSCs exist in a quiescent state and are capable of self-renewal and differentiation, and are able to perpetuate leukemic cell growth in long-term culture assays and in the murine nonobese diabetic/severe combined immunodeficiency (NOD/SCID) model system.[1–4] CD34$^+$/CD38$^-$ AML cells were shown to fulfill the criteria for LSCs *in vivo*.[5,6] Although, recent studies employed more severely immunocompromised mice found that even CD34$^-$ or CD38$^+$ AML cells in some cases were able to reconstitute AML.[7,8]

The regulation of stem cell self-renewal and differentiation requires a specific microenvironment of surrounding cells known as the stem cell niche. The concept of the stem cell niche was first proposed for the human hematopoietic system in the 1970s.[9] The HSC niche in mouse bone marrow (BM) is

What's new?

Acute myelogenous leukemia (AML) is maintained by a subset of self-renewing leukemia stem cells (LSCs). Thus, to effectively treat AML, treatments targeting LSCs are needed. AML cells expressing CD34 but not CD38 (CD34+/CD38-) contain abundant LSCs and were found in this study to express a greater amount of CD82 than CD34+/CD38+ AML cells. CD82 was further found to regulate the survival of CD34+/CD38- AML cells and their adhesion to the bone marrow microenvironment, suggesting that this glycoprotein could be an attractive target for LSC eradication.

composed of an endosteal lining of stromal cells, extracellular matrix proteins, and osteoblasts.[10–12] Specific adherens junction molecules such as N-cadherin mediate adhesion between HSCs and niche cells in the adult hematopoietic system.[11]

Recent work has shown that interaction between CXCR4 on leukemic cells and its ligand stromal cell-derived factor-1 (SDF-1) in the niche is necessary for proper homing and *in vivo* growth of leukemic cells.[13] Moreover, interaction between LSCs and the niche mediated by adhesion molecule CD44 is required for maintenance of LSCs behavior.[14] CD44 mediates adhesive cell-cell and cell-extracellular matrix interactions by binding its main ligand, hyaluronan, a glycosaminoglycan that is highly concentrated in the endosteal region.[14,15] All together, adhesion molecules play an important role in maintaining the characteristics of LSCs.

CD82/KAI-1, a member of the tetraspanin superfamily, was originally identified as an accessory molecule in T-cell activation.[16] The most well-characterized function of CD82 in nonimmune cells is integrin-mediated cell adhesion to extracellular matrix.[17] Forced expression of CD82 up-regulated tissue inhibitors of metalloproteinase 1 (TIMP1) and inactivated matrix metalloproteinases 9 (MMP9) in the H1299 human lung carcinoma cells, resulting in suppression of tumor invasion and metastasis.[18] Cell adhesion to collagen I, which is one of the major proteins in the bone marrow (BM) niche, is mostly mediated by three integrin receptors $\alpha1\beta1$, $\alpha2\beta1$, and $\alpha11\beta1$ expressed on cell surface of mesenchymal stem cells.[19] Integrin may associate with CD82 in $CD34^+/CD38^-$ AML cells to promote adhesion to the endosteal niche. However, the roles of CD82 in hematopoietic cells remain to be elucidated.

In this study, we analyzed the protein expression profile of freshly isolated $CD34^+/CD38^-$ AML cells from individuals with AML and compared it with the expression profile of their $CD34^+/CD38^+$ counterparts using isobaric tags for relative and absolute quantitation (iTRAQ) and found the aberrant expression of CD82 in $CD34^+/CD38^-$ AML cells. This study also explored the function of CD82 in $CD34^+/CD38^-$ AML cells *in vitro* as well as *in vivo* by utilizing NOD.Cg-*Rag1*^{tm1Mom} *Il2rg*^{tm1Wjl}/SzJ mice.

Material and Methods

Sample collection and isolation of $CD34^+/CD38^-$ AML cells and their $CD34^+/CD38^+$ counterparts

Leukemia cells were freshly isolated from AML patients (n = 18) with World Health Organization (WHO) classification system subtype minimally differentiated AML (case 6), AML without maturation (cases 1 and 10), AML with maturation (cases 2, 7, and 12), acute myelomonocytic leukemia (cases 4, 14, and 15), AML with myelodysplasia changes (cases 3, 5, 8, 9,16, 17, and 18), and therapy-related AML (cases 11 and 13) after obtaining informed consent with Kochi University Institutional Review Board approval (Supporting Information Table S1). The informed consent was obtained in accordance with the Declaration of Helsinki. $CD34^+/CD38^-$ AML cells and $CD34^+/CD38^+$ counterparts were purified by magnetic cell sorting utilizing a CD34 MultiSort kit and a CD38 MicroBead kit (Miltenyi Biotec GmbH, Germany), as previously described (Supporting Information Fig. S1*a*).[20]

Cells

Chronic eosinophilic leukemia (CEL) EOL-1 cells were obtained from RIKEN BRC Cell Bank (Tsukuba, Japan). Imatinib-resistant EOL-1R cell line was established by culturing with increasing concentrations of imatinib (from 1 to 100 nM) for 6 months.[21] Most of EOL-1R cells expressed CD34 ($92 \pm 9\%$) on their cell surface. On the other hand, CD34 was rarely detectable on cell surface of parental EOL-1 cells ($0.1 \pm 0.1\%$) (figure not shown).

Isolation and culture of primary mesenchymal stromal cells (MSCs)

MSCs were isolated from a BM of healthy donors. BM cells were subjected to centrifugation over a Ficoll-Hypaque gradient to separate mononuclear cells. These cells were resuspended in α-minimal essential medium (Gibco BRL, Rockville, MD) containing 20% fetal bovine serum (FBS) and plated at an initial density of 10^6 cells.[22]

Protein extraction

Proteins were extracted using the complete mammalian proteome kit (539779, Calbiochem, Darmstadt, Germany), according to the manufacturer's instructions.

iTRAQ labeling of peptides

Each protein sample (100 μg) was digested with trypsin and labeled with iTRAQ reagents (Applied Biosystems, Framingham, MA) according to the manufacturer's instructions. Briefly, the proteins extracted from $CD34^+/CD38^-$ AML cells were labeled with iTRAQ reagents 114 (case 1) or 116 (case 2), and proteins extracted from $CD34^+/CD38^+$ counterparts